




A review of breast boundary and pectoral muscle segmentation methods in computer-aided detection/diagnosis of breast mammography

Mehrdad Moghbel¹  · Chia Yee Ooi¹ · Nordinah Ismail¹ · Yuan Wen Hau² · Nogol Memari³

Published online: 29 May 2019
© Springer Nature B.V. 2019

Abstract

Mammography can be considered as the current gold standard for detecting early signs of breast cancer and is in wide use throughout the world. As confirmed by many studies, breast cancer screening using mammography can reduce breast cancer-related mortality by 30–70%. However, although the interpretation of mammography images by a second reader has been shown to increase the cancer detection rate, this practice is not widespread due to the cost associated. As a result, computer-aided detection/diagnosis (CAD) of breast mammography has been gaining popularity with various studies illustrating the positive effects of using computers in detecting early breast cancer signs by providing the radiologists with a second opinion with most of these CAD systems requiring the breast outline and pectoral muscle regions (in images acquired using Medio-Lateral-Oblique view) to be segmented from mammograms prior to the classification. This paper discusses recent developments and methods proposed for segmenting the breast and pectoral muscle regions and compares the performance and shortcomings of different approaches grouped together based on the techniques used. While it is arduous to compare these methods using comparative analysis, a set of common performance evaluation criterion is defined in this study and various methods are compared based on their methodology and the validation dataset used. Although many methods can achieve promising results, there is still room for further development, especially in pre-processing and image enhancement steps where most methods do not take the necessary steps for ensuring a smooth segmentation of boundaries. In this paper, the most effective pre-processing, image enhancement and segmentation concepts proposed for breast boundary and pectoral muscle segmentation are identified and discussed in hopes of aiding the readers with identifying the best possible solutions for these segmentation problems.

✉ Mehrdad Moghbel
mehrdad2275@gmail.com

¹ Malaysia-Japan International Institute of Technology, Universiti Teknologi Malaysia, 54100 Kuala Lumpur, Malaysia

² School of Biomedical Engineering and Health Sciences, Universiti Teknologi Malaysia, 81310 Johor Bahru, Johor, Malaysia

³ Department of Computer and Communication Systems, Faculty of Engineering, Universiti Putra Malaysia, 43400 Serdang, Selangor, Malaysia

Keywords Breast mammography · Image segmentation · Breast segmentation · Pectoral muscle segmentation · Computer-aided detection/diagnosis

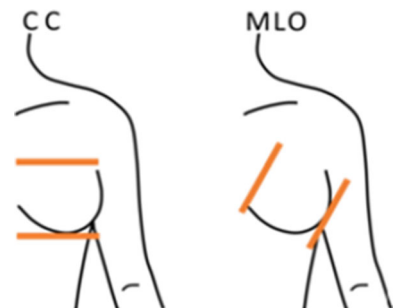
1 Introduction

Breast cancer can be considered as one of the most common global health problems and is considered as the second cause of cancer-related mortalities in women (Kwan et al. 2009). With the potential of affecting women over the age of 15 (and most commonly seen in women between the ages of 35 and 55) and men (most commonly seen over the age of 40), breast cancer is responsible for over 150,000 deaths per year (Senthilkumar and Umamaheshwari 2011). Considering the high mortality rates and the fact that cancer cells can double in size in a period of 3 to 9 months (Collins 1956), early diagnosis and treatment planning can be considered as an important aspect of ensuring favorable prognosis of the patient (Deserno et al. 2011). Breast mammography using low-dose X-ray imaging is considered one of the most effective methods for detecting breast cancer in the population with many screenings done at various examination centers around the world. Mammography is also a popular screening procedure (alongside ultrasound examination) for asymptomatic (patients with no clinical signs of cancer) and/or at risk populous where it has been shown to reduce the breast cancer-related mortality rate by 30–70% (Linguraru et al. 2006).

Although the mammography procedure was initially based on radiography films (known as film-based mammography), the recent introduction of digital mammography known as full-field digital mammography (FFDM) has further reduced the imaging time and has made image storage/transmission easier and more efficient with studies showing that there is no significant difference in their diagnostic accuracy (Lewin et al. 2001). In digital mammography, a detector array is used in place of traditional X-ray absorbing film resulting in digital images, enabling easy changes in image orientation, magnification, contrast and brightness as required by the examining radiologist after the image acquisition. Digital mammography is gaining popularity as it is cheaper to operate and images can be easily stored digitally as Digital Imaging and Communications in Medicine (DICOM) files. Usually, the image of the breast is acquired using two projection planes during the mammography procedure namely Cranio-Caudal (CC) and Medio-Lateral-Oblique (MLO) planes, as illustrated in Fig. 1.

Taken at an angle, Medio-Lateral-Oblique (also referred to as the side view) aims to capture the entire breast and often includes the lymph nodes with the pectoral muscle usually visible at the upper portion of the image. Taken from top to bottom, the Cranial–Caudal aims to capture the medial portion as well the external lateral region of the breast as much as possible. Examples of mammography images taken at these views are illustrated in Fig. 2.

Fig. 1 Direction used for acquiring Cranial–Caudal (CC) and Medio-Lateral-Oblique (MLO) breast mammograms



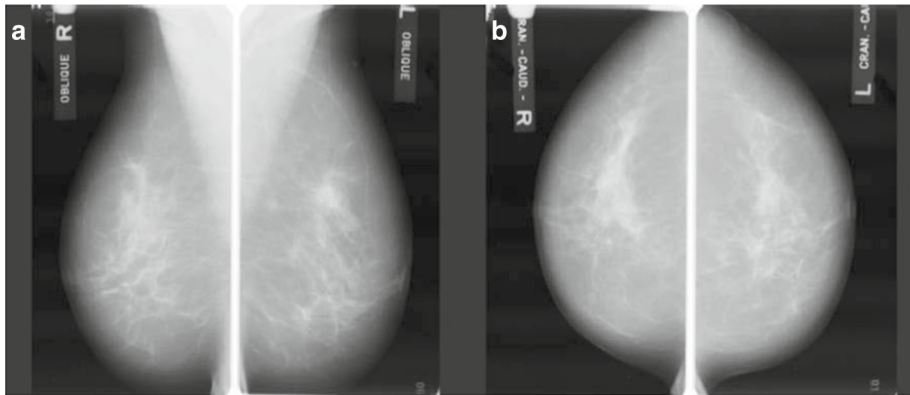


Fig. 2 Mammography images acquired at different projections. **a** MLO and **b** CC mammograms

The acquired mammography images are often examined by a specialist radiologist who will identify and locate any abnormalities in the patient's breasts. However, as these radiologists often have to inspect many patients on a daily basis, there is a high rate of false negatives and misdiagnosis due to fatigue coupled with inherent difficulties associated with reading mammography images, i.e. complexity of breast tissue structure and subtle nature of cancer during early development stages. In fact, studies have shown that approximately 10 to 30% of cancers are missed during the examination (Christoyianni et al. 2002; Marx et al. 2004; Elshinawy et al. 2010). To improve the radiologist's performance and/or to provide a second opinion during the examination, the use of computer-aided detection/diagnosis (CAD) has been proposed by many researchers and is adopted by many breast imaging centers as studies have shown that the performance of the radiologist can be improved by utilizing CAD in their evaluation (Sampat et al. 2005; Doi 2007). Using digital image processing techniques, CAD tries to detect abnormalities in mammography images (such as calcifications and masses) and then classifies the images based on detected abnormalities using machine learning methods (Tang et al. 2009). Moreover, apart from the classification, the CAD system can also be used for locating possible abnormalities and highlighting them to the radiologist. The computer system capable of classifying medical images is known as computer-aided diagnosis (CADx) and the system that is used for highlighting abnormalities in the image is known as computer-aided detection (CADe). Although these systems can be separated, majority of designs combine CADe and CADx into a single solution commonly referred to as CAD. It should be noted that CAD systems are designed based on a specific medical purpose, i.e. a CAD system designed for evaluating breast images using mammography will not function correctly on breast images acquired using ultrasound imaging. Unlike some other breast-related CAD approaches such as the CAD systems based on breast thermography (Moghbel and Mashohor 2013), there are some commercially available mammography CAD systems that are in use in hospitals and clinics such as iCAD (Zhang et al. 2007) and ImageChecker (Senthilkumar and Umamaheshwari 2011).

Traditionally, mammography-based breast CAD systems are comprised of pre-processing, localization and/or segmentation, feature extraction and classification steps. However, recently introduced deep learning-based methods usually combine feature extraction and classification into a single step. Pre-processing steps are often used for enhancing the image where the desired image features are emphasized and unwanted features are de-emphasized regardless of the machine learning method used. Image enhancement and breast region seg-

mentation can be considered as the main steps in most CAD systems as defining a proper region of interest (ROI) can increase the CAD accuracy by enhancing the anatomical features desired while removing any unwanted regions. Determining the breast boundary is important as it is used for removing background objects such as scanning labels and artifacts along with correcting the position of the breast as the screen-film mammography (SFM) is often not positioned correctly in the scanner during the digitization process. Segmentation and removal of the pectoral muscle from mammography images captured using the MLO plane is of high value as the CAD systems could easily misclassify the pectoral muscle region as fibroglandular tissues (due to similar image characteristics). Moreover, the pectoral muscle region is often examined by the radiologist (and some CAD systems) for signs of abnormal axillary lymph (as an indication for the presence of occult breast carcinoma) as many cancers can develop in this area and its examination can lead to reduced false negative findings (Kwok et al. 2001).

In this review, as an expansion of previous reviews by Mustra et al. (2016) and Ganesan et al. (2013), different breast region and pectoral muscle segmentation methods (from MLO images) in both full-field digital mammography and digitized screen-film mammography images are discussed and compared based on the image processing techniques utilized. A comparison between the performances of these methods is presented in this study. Since the majority of proposed segmentation methods are tested and validated using publicly accessible DDSM and MIAS datasets, this comparison can be used to identify the best-performing methods from the literature. Furthermore, the best performing pre-processing, image enhancement and segmentation methods are identified and discussed for familiarizing the reader with the best performing techniques. Although the majority of methods discussed are capable of achieving good segmentation accuracy, there is still room for further improvements especially in pre-processing and image enhancement steps where most methods omit the necessary steps for ensuring a smooth segmentation of boundaries. The rest of the paper is organized as follows. Section 2 describes the methodology adopted in this paper for comparing different segmentation methods along with mammography acquisition procedures and performance measures used in this study. Section 3 presents a review of publicly accessible mammography datasets. Section 4 presents a review of breast region segmentation methods grouped based on their use of different image processing concepts. Section 5 presents a review of pectoral muscle segmentation methods from MLO-mammograms grouped based on their use of different image processing concepts. Section 6 presents a discussion on various methods reviewed in this study and identifies the most prominent pre-processing and segmentation concepts and Sect. 7 draws the conclusion.

2 Research methodology

In this study, PubMed and Google Scholar search engines were utilized for finding articles containing breast and/or pectoral muscle segmentation methods based on the keywords: “segmentation of pectoral muscle region | boundary in mammograms | mammography, detection of pectoral muscle region | boundary in mammograms | mammography, segmentation of breast region | boundary in mammograms | mammography, detection of breast region | boundary in mammograms | mammography” up to the first week of February 2019 without any limitation on article type and the date of publication with ‘|’ denoting ‘or’ in the search terms used. Journal articles and conference proceedings along with book chapters written in English were retained while letters to the editor, thesis and short communications were

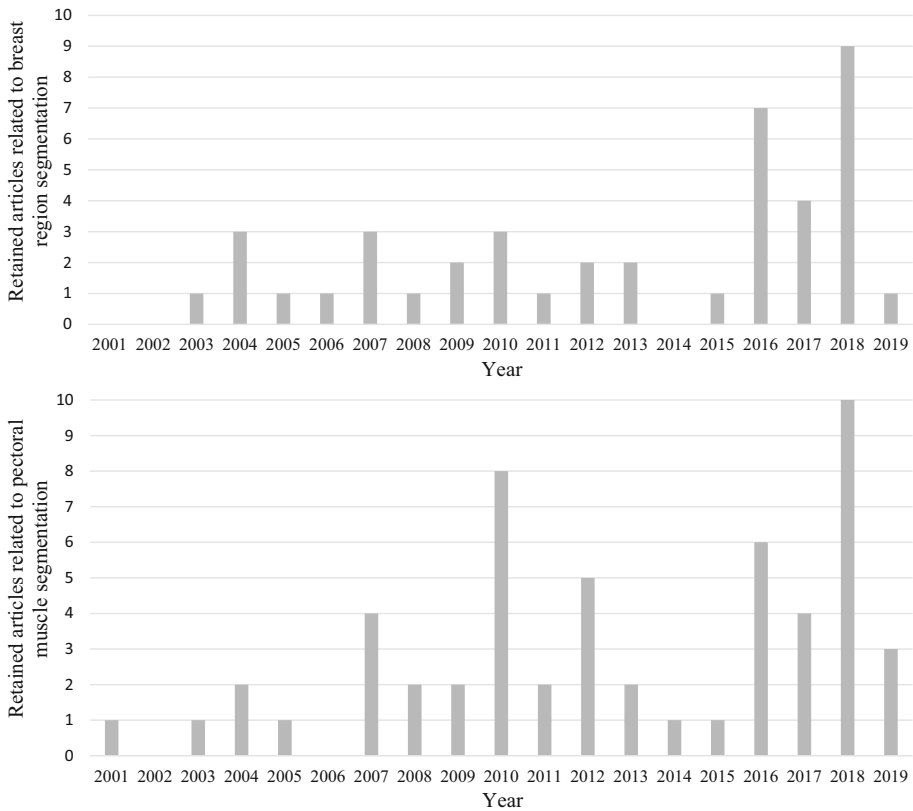


Fig. 3 The number of retained articles related to the breast region and pectoral muscle segmentation

excluded from the study. A first selection of the retained articles was done by reading the title and abstract where studies not related to breast and/or pectoral muscle segmentation were removed. The selected manuscripts were further screened and those without a clearly described methodology section were removed. Additionally, some manuscripts that were missed during the database search were retrieved based on the reference list of other selected articles. The selected manuscripts and the corresponding references were stored in EndNote X9 reference manager. In total, 20 journal articles, 19 conference proceedings and 3 book chapters discussing the breast segmentation and 31 journal articles, 20 conference proceedings and 4 book chapters discussing the pectoral muscle segmentation were retained in this review with Fig. 3 illustrating the statistics of these selected papers. The majority of papers referenced in this review were published during the last 5 years, mainly due to the development of computational capability and a recently renewed interest in CAD systems designed for detecting breast cancer.

2.1 Classification of image segmentation techniques

All image segmentation techniques discussed in this study can be classified based on the amount of shape information incorporated by the method. The more an algorithm utilizes shape related information, the more specialized the algorithm becomes. As an example, a

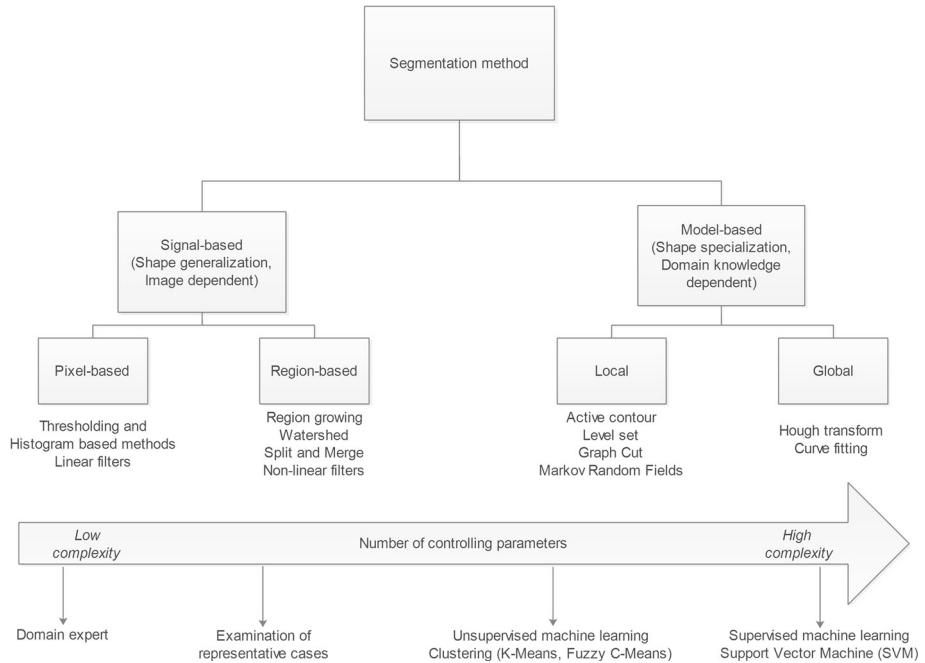


Fig. 4 Overview of segmentation methods discussed in this review

simple threshold-based technique can be used for segmenting any shape with pixels that contain similar properties (i.e. intensity). In contrast, a deformable model-based method designed and optimized for pectoral muscle segmentation might function poorly if applied to other problems such as breast boundary segmentation. An overview of various segmentation methods discussed in this review is illustrated in Fig. 4.

The methods on the left (i.e. histogram-based methods that are low in complexity) use the least shape information and as a result, can be applied in a wide range of applications as these methods could be optimized using a few parameters as they do not incorporate a high degree of domain specific knowledge. While optimizing and implementing these methods, it is often enough to examine some representative cases for determining the overall segmentation requirements or to consult a domain expert (i.e. a radiologist). On the other hand, the methods to the right (i.e. non-linear Hough transform based methods that are high in complexity) often require an extensive optimization and parameter selection steps as they incorporate a large amount of domain specific knowledge and can be considered as a specialized method. The number of adjustable parameters in a segmentation method increases with the amount of shape/domain knowledge utilized with complex segmentation problems often solved using a whole pipeline of different segmentation methods belonging to different concepts. In such a case, the method is usually classified based on the algorithm using the most domain-specific knowledge, an approach using thresholding for initial segmentation and a model-based method for refining this initial segmentation is considered as a model based method.

2.2 Evaluating the performance of segmentation methods

2.2.1 Definitions of true and false positive/negative

- True positive (TP): ROI pixel correctly segmented as ROI pixel
- False positive (FP): Non-ROI pixel segmented as ROI pixel
- True negative (TN): Non-ROI pixel correctly segmented as non-ROI pixel
- False negative (FN): ROI pixel segmented as non-ROI pixel

2.2.2 Sensitivity and precision

Sensitivity (also called positive predictive value) and precision (also called recall) represent the probability that the segmentation method will correctly identify ROI pixels. Written in percent, this value is 100 for a perfect segmentation while any decrease in this value correlates to an increased discrepancy between segmentation and ground truth with 0 as the lowest possible value. Sensitivity is computed as:

$$\text{Sensitivity} = \frac{\text{total TP}}{\text{total TP} + \text{total FN}} \times 100 \quad (1)$$

Precision is computed as:

$$\text{Precision} = \frac{\text{total TP}}{\text{total TP} + \text{total FP}} \times 100 \quad (2)$$

2.2.3 Accuracy

Accuracy, expressed in percent, represents the overall performance of a segmentation method. Accuracy is computed as:

$$\text{Accuracy} = \frac{\text{total TP} + \text{total TN}}{\text{total TP} + \text{total FP} + \text{total TN} + \text{total FN}} \times 100 \quad (3)$$

2.2.4 Volumetric overlap

Volumetric overlap (VO), expressed in percent, represents the number of pixels in the intersection of segmented region (A) and the ground truth (B) divided by the number of pixels in the union of A and B. This value is 100 for a perfect segmentation while any decrease in this value correlates to increased discrepancy between segmentation and ground truth with 0 as the lowest possible value, when there is no overlap at all between segmentation and reference. It can be calculated in percent from the following formula:

$$\text{VO} = \frac{|A \cap B|}{|A \cup B|} \times 100 \quad (4)$$

2.2.5 Dice similarity coefficient

Dice similarity coefficient (DSC) represents the overall performance of the algorithm in correctly including the pixels of the ROI inside the segmentation. A value of 0 represents no overlap between the segmented region (A) and ground truth (B) while a value of 1 represents perfect segmentation.

It can be calculated by the following formula:

$$DSC = \frac{2|A \cap B|}{|A| + |B|} \quad (5)$$

2.2.6 Jaccard similarity coefficient

Jaccard similarity coefficient (JSC) represents the overall performance of the algorithm in correctly including the pixels of the ROI inside the segmentation. A value of 0 represents no overlap between the segmented region (A) and ground truth (B) while a value of 1 represents perfect segmentation. It can be calculated by the following formula:

$$JSC = \frac{2|A \cap B|}{|A \cup B|} \quad (6)$$

It should be noted that the jaccard similarity coefficient is often excluded from the studies as it can be computed from the dice similarity coefficient using the following formula:

$$JSC = \frac{DSC}{2 - DSC} \quad (7)$$

2.3 Assessing the density of mammography images

The density of mammography images is routinely assessed using Breast Imaging Reporting and Data System (BIRADS) guidelines proposed based on the difference in the ratio of fat and glandular tissues inside the breast (D'orsi et al. 1998). It should be noted that BIRADS is different from BI-RADS guidelines that are aimed at standardizing mammography image assessment by proposing a specific set of guidelines for categorizing (6 categories) abnormalities in mammography images. There are two versions of the BIRADS guidelines, original guidelines proposed in 2003 and updated guidelines proposed in 2013. While they differ on guideline definitions, they fundamentally represent the same conditions as shown in Table 1.

Generally, the dense breasts with small abnormalities or with abnormalities located deep inside the breast are the most difficult to assess and categorize. In such cases, the radiologist might request additional mammograms using different views to help with the diagnosis. Moreover, younger patients tend to have denser breasts making it more difficult to assess their mammograms. Figure 5 illustrates the different BIRADS categories.

3 Publicly accessible mammography datasets

Having a large heterogenic dataset with a high number of images is a prerequisite for developing an unbiased solution in most medical problems. Current public mammography image datasets include Mammographic Image Analysis Society (MIAS)/Mini-MIAS, Digital Database for Screening Mammography (DDSM)/CBIS-DDSM, INbreast (solely comprised of FFDM images), BancoWeb, INbreast and Breast Cancer Digital Repository (BCDR) datasets. As the INbreast dataset is no longer being maintained in any repository, access is difficult as the dataset can be (currently) accessed by e-mailing the dataset curator but it is unclear how long this dataset will be available. On the other hand, BancoWeb dataset (Matheus and Schiabel 2011) does not come with ground truth segmentation and detailed

Table 1 BIRADS density categories and assessment guidelines

BIRADS category	Definition	Assessment guidelines proposed in 2003	Assessment guidelines proposed in 2013
I (a)	Fatty breast	Breast tissue is mostly comprised of fat with glandular tissue making less than 25% of the total breast tissue	Breast tissue is mostly comprised of fat
II (b)	Scattered fibroglandular tissue	Fibroglandular tissue making 25–50% of the total breast tissue	Scattered fibroglandular tissue in some areas of the breast
III (c)	Heterogeneously dense breast	Fibroglandular tissue making 50–75% of the total breast tissue with fibroglandular tissue scattered throughout without forming any clusters	Fibroglandular tissue scattered throughout without forming any clusters
IV (d)	Dense breast	Fibroglandular tissue making more than 75% of the total breast tissue often resulting in reduced diagnosis sensitivity	Extremely dense breast

information regarding the location and type of suspicious regions (apart from few images) that greatly limits the usability of this dataset (as it has not been used in any breast boundary and pectoral muscle segmentation studies). Unfortunately, as is the case with most other medical image datasets, publicly accessible mammography datasets are still limited.

3.1 Digital Database for Screening Mammography

Digital Database for Screening Mammography (DDSM) and its updated version known as the Curated Breast Imaging Subset of DDSM (CBIS-DDSM) are one of the benchmark datasets and are being used for development of many breast CAD systems (Heath et al. 1998; Clark et al. 2013). This dataset contains 2620 studies totaling 10,480 SFM images with both MLO and CC views provided for each study. For each suspicious image containing lesions, pixel-level ground truth segmentation and information regarding the location and type of suspicious regions are provided along with BI-RADS and BIRADS categories. While DDSM dataset images come in JPEG image format which is difficult to process and work with (as the compression codec used is not supported in most mainstream data analysis applications), the images in CBIS-DDSM dataset are provided in 16-bit DICOM format with a resolution of 3131×5295 pixels (width \times height). Figure 6 illustrates some sample images from CBIS-DDSM dataset.

3.2 Mammographic Image Analysis Society dataset

Mammographic Image Analysis Society (MIAS) dataset includes 161 studies totaling 322 SFM images captured using MLO view during the United Kingdom National Breast Screen-

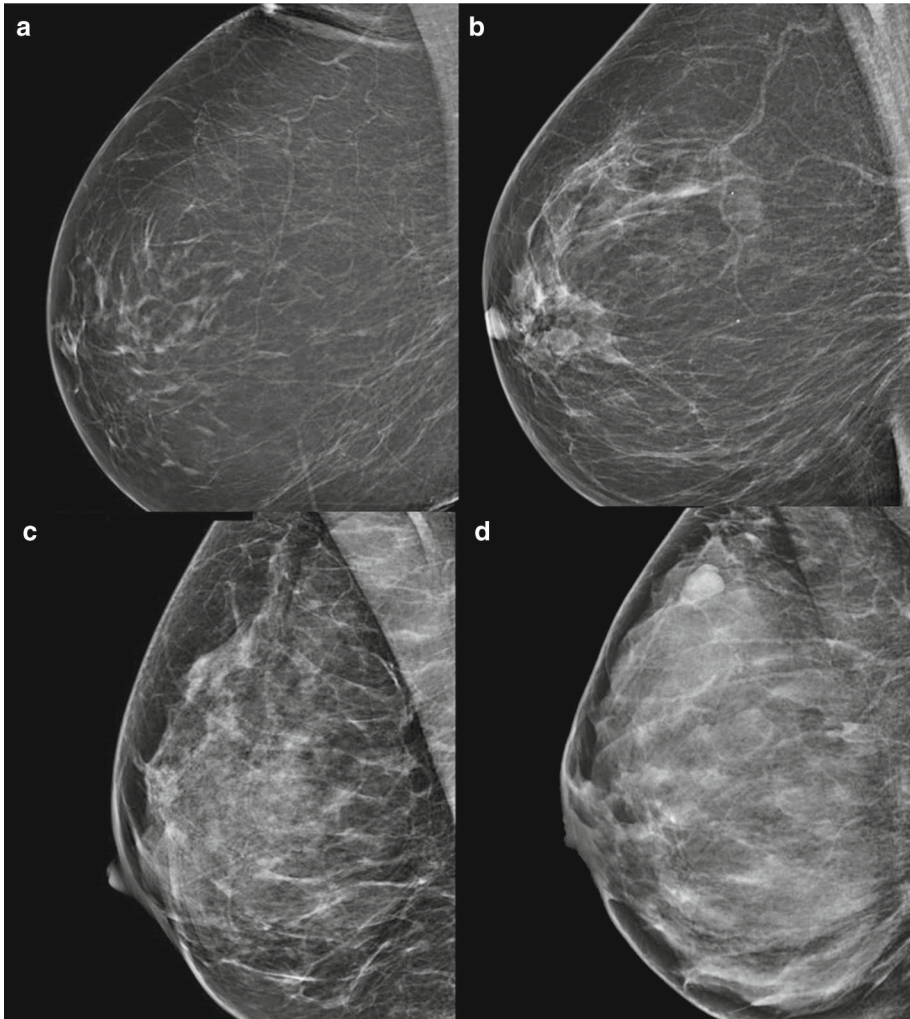


Fig. 5 Different BIRADS classes. **a** BIRADS I, **b** BIRADS II, **c** BIRADS III and **d** BIRADS IV mammograms

ing Program (Suckling et al. 1994). The mini-MIAS dataset is an improvement of the MIAS dataset where the images are clipped and padded so that all the images have a resolution of 1024×1024 pixels and are provided as 8-bit (256 distinct intensity levels) PGM files. Unfortunately, this dataset does not contain pixel-level ground truth segmentation and detailed information regarding the location and type of suspicious regions with different types of abnormalities (calcifications, well-defined speculated or ill-defined masses, architectural distortion or asymmetry) along with the cancer categories (benign or malignant) and breast boundaries being provided. The images in MIAS and mini-MIAS datasets come in PGM format which is easy to process and work with, Fig. 7 illustrates some sample images from MIAS and mini-MIAS datasets.

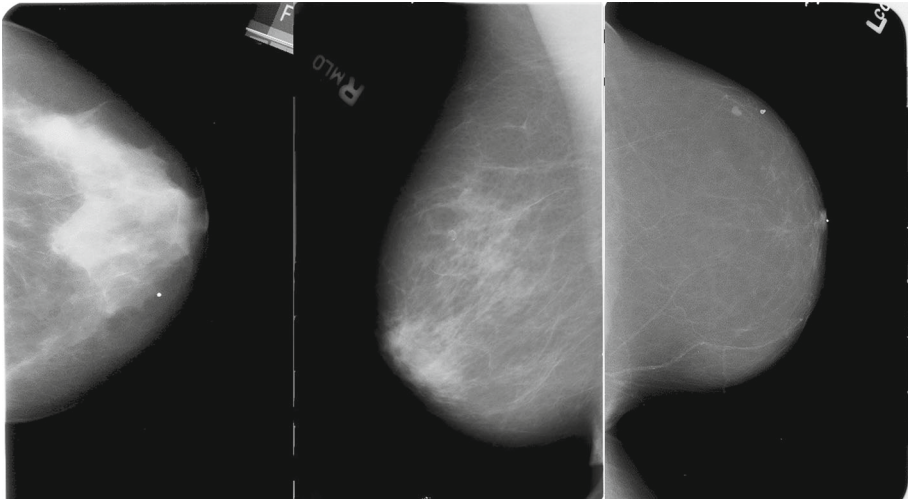


Fig. 6 Sample images from CBIS-DDSM dataset

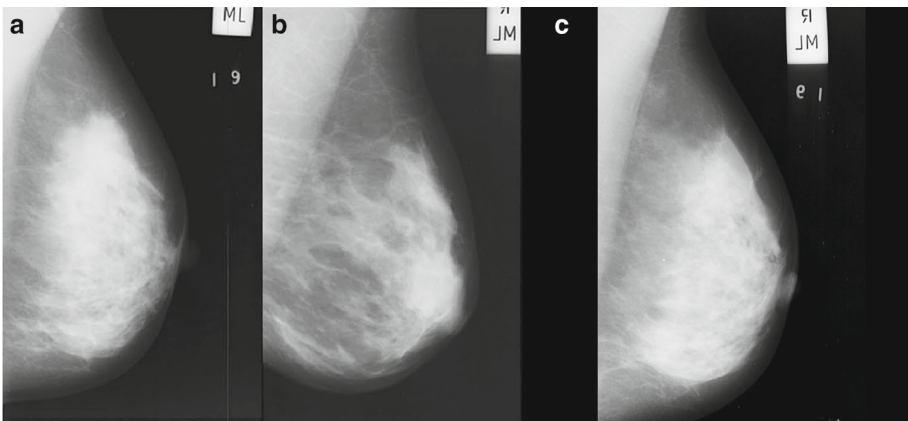


Fig. 7 Sample images from **a**, **b** MIAS and **c** mini-MIAS datasets

3.3 Breast Cancer Digital Repository dataset

Breast Cancer Digital Repository (BCDR) is one of the newer SFM datasets with the potential of becoming a benchmark dataset for development of CAD systems containing 1125 studies totaling 3703 images with MLO and CC views included for each study provided as 8-bit TIFF images with a resolution of 720×1168 pixels (Lopez et al. 2012). For each image, pixel-level ground truth segmentation and information regarding the location and type of suspicious region are provided along with the BI-RADS categories. Images in the BCDR dataset come in 8-bit TIFF format which is easy to process and work with, Fig. 8 illustrates some sample images from BCDR dataset. Moreover, a companion dataset (to BCDR) exclusively comprised of FFDM data known as BCDR-DM is in development that currently contains 1042 studies totaling 3612 images provided as 14-bit TIFF images with a resolution of 3328×4084 or 2560×3328 pixels (according to the patient's breast size). For some images in the

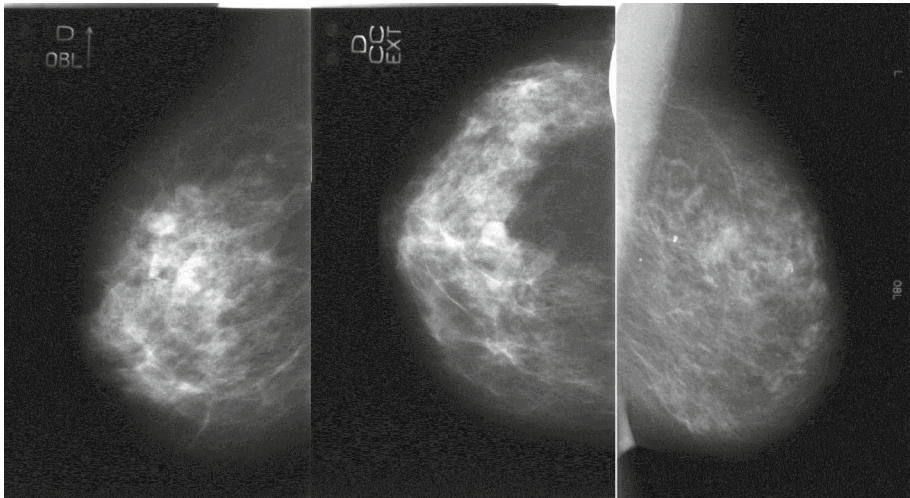


Fig. 8 Sample images from BCDR dataset

dataset, the ground truth segmentation and information regarding the location and type of suspicious regions are provided along with BI-RADS and BIRADS categories. It should be noted as the BCDR-DM dataset is currently in active development, new studies are added routinely along with ground truth segmentation and other information for images already in the dataset. Upon completion, BCDR-DM dataset could become the new benchmark dataset (along with the CBIS-DDSM) for developing breast related CAD systems as the number of images and better quality of FFDM images makes this dataset ideal for developing CAD systems.

3.4 Inbreast dataset

The Inbreast dataset is entirely comprised of 14-bit DICOM images captured using FFDM and is provided with a resolution of 3328×4084 or 2560×3328 pixels (according to the patient's breast size). The dataset contains a total of 115 studies where 90 studies come with both MLO and CC views (of each breast) and 25 studies are from mastectomy patients (two images per case), totaling 410 images (Moreira et al. 2012). For each image, pixel-level ground truth segmentation and information regarding the location and type of suspicious region, image orientation and anatomical structures are provided along with the BIRADS categories. The Inbreast dataset has the potential of becoming a benchmark dataset for the development of CAD systems (if the dataset is maintained in a repository and made more accessible to researchers). Figure 9 illustrates some sample images from INbreast dataset.

4 Breast boundary detection and segmentation

As mentioned, mammography images (digitized SFM images in particular and some non-DICOM FFDM images) often contain various background objects such as labels and markers that need to be removed. As FFDM images do not include any labels (although they might include small artifacts), they can be segmented by a thresholding approach with ease as the

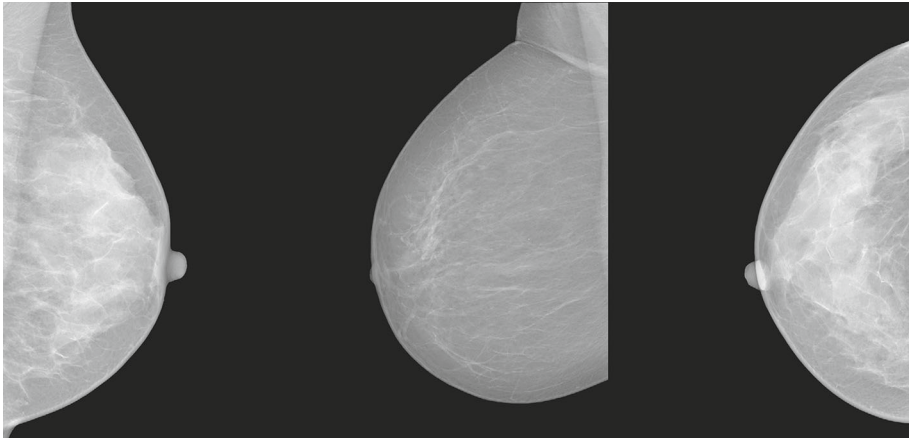


Fig. 9 Sample images from INbreast dataset

method proposed by Mustra et al. (2009) was able to achieve an accuracy of 100% in segmenting the breast outline using FFDM images. Moreover, digitized film-based mammography images are often scanned with varying orientation and the breast is often not positioned correctly in the scanner (at the edge of the scanner frame), as illustrated in Fig. 10. It should be noted that as the breast is a 3D structure captured using mammography (2D imaging modality), different tissues can overlap causing different attenuation (intensity) levels in the absorption of passing X-rays. Another factor influencing the segmentation performance of any given method is the variations in mammogram's quality and patient's breast density. Different patients have different breast densities where these densities can greatly affect the performance of any segmentation method. As a result, relying on a global intensity threshold as the sole segmentation method does not often result in a properly segmented breast boundary, especially in SFM images.

4.1 Thresholding methods

Thresholding can be considered as one of the earliest and simplest methods proposed for the segmentation of images and is based on the notion that pixels over or under a certain intensity value (threshold) can be assigned to the foreground and the rest of the pixels assigned to the background. Thresholding an image can be done using either a global or local approach. In a global thresholding approach, a single threshold value is computed for the entire image that can make accurate segmentation of images with extensive intensity variations difficult. In local thresholding approach, the image is often decomposed to a series of non-overlapping windows with a threshold value for each window computed with thresholding method proposed by Otsu (Otsu 1979) being the most popular thresholding approach as it can produce good results in wide range of images (with large variations in intensity). It should be noted that evolutionary computing methods such as genetic algorithm and particle swarm optimization-based thresholding methods are becoming more popular as they can provide good segmentation accuracy in a wide range of images. As the thresholding-based methods often cannot segment the boundaries smoothly (especially in SFM images), some thresholding-based approaches also include boundary smoothing techniques (mostly implemented using mathematical morphology) as their post-processing steps.

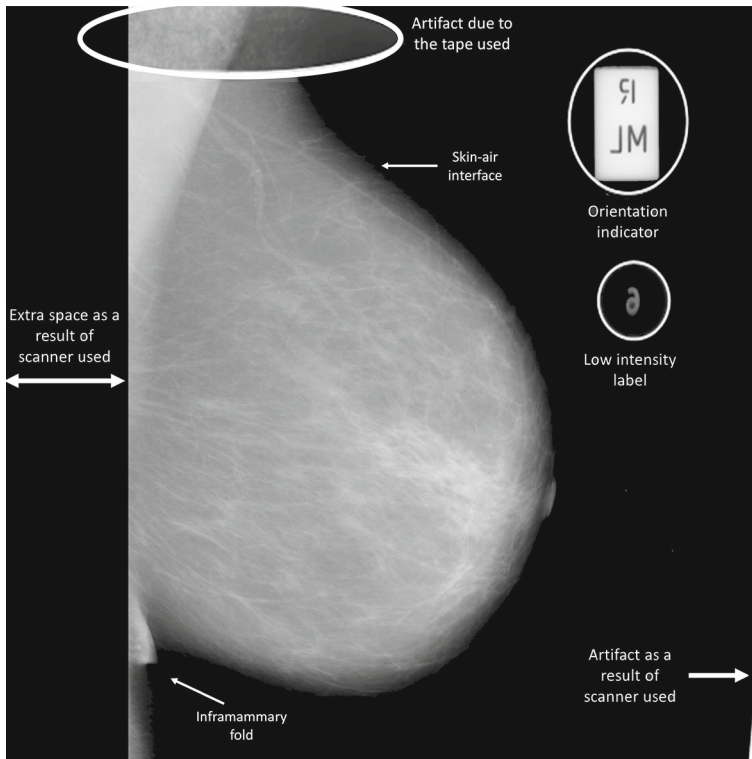


Fig. 10 Scanning artifacts and labels on a sample digitized mammography image

Qayyum and Basit (2016) proposed using Otsu's thresholding method for extracting the breast boundaries where the images are first filtered using median filtering followed by thresholding and morphological operations for removing small background objects such as labels. The object having the highest number of connected pixels is then taken as the breast region. Evaluated using the mini-MIAS dataset based on visual inspection of the accuracy of the segmentation, their proposed method was able to provide good and acceptable segmentation in 96.89% and 2.48% of the images, respectively. A similar approach was also proposed by Shinde and Rao (2019), Shen et al. (2018) and Toz and Erdogmus (2018) with their results validated using visual inspection of the accuracy of the segmentation without any detailed statistical performance measures provided. The method proposed by Salama et al. (2018) is also based on a similar approach with their method using a 5×5 median filtering of the images (for noise reduction) prior to thresholding without providing any detailed statistical performance measures. Esener et al. (2018) also proposed a similar approach with their method utilizing adaptive median filtering of the images (for better noise reduction) prior to thresholding using Otsu's thresholding method without any detailed statistical performance measures provided. The method proposed by Ancy and Nair (2018) is also based on a similar approach with their method adding a contrast enhancement step using Gamma correction prior to thresholding without providing any detailed statistical performance measures. In the thresholding approach proposed by Mirzaalian et al. (2007), the image is first filtered using a low-pass filter. Then, the image is thresholded at the knee of the cumulative histogram and the breast is segmented by taking the object with the highest number of connected pixels.

They too validated their results using visual inspection of the accuracy of the segmentation without providing any detailed statistical performance measures. Ergin et al. (2016) proposed a thresholding approach for extracting the breast boundaries in mammograms. In their proposed methods, the images are filtered using median filtering followed by thresholding and morphological operations for removing small background objects such as labels. Finally, the breast region is segmented by taking the object with the highest number of connected pixels. They validated the results of their proposed methods using visual inspection of the accuracy of the segmentation without providing any detailed statistical performance measures. A similar thresholding-based approach for extracting the breast boundaries using images from the mini-MIAS dataset was proposed by Bajaj et al. (2017) where the images are segmented using a thresholding approach followed by morphological operations for removing small background objects such as labels and scanning artifacts. Similar to other methods, the breast is segmented by taking the object with the highest number of connected pixels. They also validated their results using visual inspection of the accuracy of the segmentation without providing any detailed statistical performance measures.

Nagi et al. (2010) proposed a global thresholding approach for extracting the breast boundaries where the images used in their study are rescaled to 8-bits and converted to binary using a fixed threshold value of 18 followed by morphology-based filtering operations for removing small background objects such as labels. As with other thresholding based methods, the object having the highest number of connected pixels is taken as the breast region. They too validated the performance of their proposed method using visual inspection of the accuracy of the segmentation without using any statistical performance measures. Palkar and Agrawal (2016) proposed a similar global thresholding-based method for extracting the breast boundaries using a fixed threshold value of 32 with the images filtered using a median filter. They also validated their results using visual inspection of the accuracy of the segmentation without providing any detailed statistical performance measures. Ibrahim et al. (2016) also proposed a similar approach using a fixed threshold value of 18 with their results validated using visual inspection of the accuracy of the segmentation without the use of any statistical performance measures. A similar approach using a fixed threshold value of 50 was proposed by Unni et al. (2018) with their results also validated using visual inspection of the accuracy of the segmentation without the use of any statistical performance measures. A global thresholding approach for extracting the breast boundaries was also proposed by Sasikala and Ezhilarasi (2018) where the images used in their study are rescaled to 8-bits with the image noise reduced using median filtering and the image contrast enhanced using Contrast-limited Adaptive Histogram Equalization (CLAHE) method. The images are then converted to binary using a fixed threshold (undisclosed) value followed by morphology-based filtering operations for removing small background objects such as labels. As with other thresholding based methods, the object having the highest number of connected pixels is taken as the breast region. They too validated the performance of their proposed method using visual inspection of the accuracy of the segmentation without using any statistical performance measures. Selvathi and Poornila (2018) proposed a global thresholding approach for extracting the breast boundaries where the images are converted to binary using a fixed threshold value of 18 and the object having the highest number of connected pixels is taken as the breast region. The breast boundary is then smoothed using morphology-based filtering operations utilizing a disc structuring element with a radius of 5 pixels. They too validated the performance of their proposed method using visual inspection of the accuracy of the segmentation without using any statistical performance measures.

Maitra et al. (2012) proposed a thresholding approach for segmenting the breast boundary where the mammograms are first enhanced utilizing CLAHE method and then segmented

using thresholding. Evaluated using the mini-MIAS dataset, their proposed method was able to achieve an accuracy of 95.7%. The thresholding method proposed by Quellec et al. (2016) starts by smoothing the images using a large median filter followed by thresholding and morphological operations for removing small background objects and smoothing the segmented boundaries with the object having the highest number of connected pixels is taken as the breast region. They too validated their results using visual inspection of the accuracy of the segmentation without providing any detailed statistical performance measures. Mustra and Grgic (2013) proposed a thresholding method for extracting breast boundaries using mammography images. First, morphological operations are used for removing small background objects such as labels. Then, the skin-air interface around the breast boundary is separated into small blocks with the separated blocks transformed into the polar coordinate system as it was hypothesized the breast boundary can be represented in more detail using the polar coordinate system. Each block is then thresholded separately (adaptive thresholding) and the breast boundary is segmented. Evaluated using the mini-MIAS dataset, their proposed method was able to achieve a VO of 96.3% and an accuracy of 99.1%.

4.2 Geometric deformable model and level set based methods

Geometric deformable models, commonly known as active contours (sometimes referred to as snakes), proposed by Caselles et al. (1997) and level sets proposed by Osher and Fedkiw (2006) work by tracking by dynamic variations along the ROI boundary and have become highly popular for segmenting medical images. Unlike active contours where a parametric characterization of contours is utilized, level set methods (Chan and Vese 2001) utilize a time-dependent partial differential equation (PDE).

Wirth and Stapinski (2003) proposed using active contours for segmenting the breast boundaries. However, their method adapts a semi-automatic approach, requiring the user to provide the approximated initial breast contour, making it a time-consuming method. Moreover, their achieved segmentation accuracy can be considered not representative of the overall accuracy of their proposed approach as they have only used 25 images from the MIAS dataset, achieving a VO of 97%. Rampun et al. (2017) proposed using an active contour without edges technique (Chan and Vese 2001) for segmenting the breast boundary. First, the image noise is reduced using a 9×9 median filtering followed by an anisotropic diffusion filter. Then, the initial breast region is approximated by thresholding the mammogram using Otsu's method and keeping the object with the highest number of connected pixels. Finally, the image entropy is computed using a 9×9 window with this entropy being used (instead of the original image) for computing the breast boundary using the active contours without edges. Evaluated on the MIAS dataset, their proposed method was able to achieve a DSC of 0.988 and an accuracy of 98.4%.

Ferrari et al. (2004a) proposed an automatic active contour-based breast segmentation method where the images are first filtered using logarithmic operation-based contrast enhancement with the images thresholded using Lloyd–Max quantizer (Scheunders 1996) followed by the morphological filtering of the image for removing small, background objects such as labels. Then, an initial breast boundary contour is estimated using the binary breast mask based on the chain-code technique coupled with histogram analysis for locating pixels along the initial breast boundary. Finally, the breasts are segmented using an active contour model based on the initial boundary. Evaluated on a subset of 84 images from the MIAS dataset, their proposed method was able to achieve a FP rate of $0.41 \pm 0.25\%$ and a FN rate of $0.58 \pm 0.67\%$. Martí et al. (2007) proposed using a contour growing (a variation of active

contours) approach for segmenting the breast boundary in mammography images. Although the achieved accuracy is considered acceptable, their proposed method had difficulties in estimating the initial contour points in dense breasts with non-uniform intensity distribution, resulting in under-segmentation of the breast boundary. Initial breast region boundary is first extracted by an edge detection algorithm applied to the mammograms filtered by a Gaussian smoothing filter using different scales. Then, initial seed points are selected using a least median error estimation approach applied to the seed candidates computed by converting the image to a gradient (in the scale space) and taking the first local maxima along the x -axis at half the image height with refinements along the y -axis. Finally, a set of candidate points for the contour growing are obtained (in a normal line along the gradient direction) and the breast boundary is segmented. Evaluated using a subset of 65 images from the MIAS dataset and 24 images from the DDSM dataset, their proposed method was able to achieve an average sensitivity and precision of 96%.

Zhou et al. (2017) proposed using a two-phase level set approach (Chan and Vese 2001) for segmenting the breast boundaries. The initial breast region is estimated by thresholding the image and keeping the object with the highest number of connected pixels. Then, the breast region is refined using a two-phase level set approach that is designed to separate the image into two regions (the breast region and background). Evaluated on the MIAS dataset, their proposed method was claimed to achieve good performance based on visual inspection of the accuracy of the segmentation. Yapa and Harada (2008) proposed using a fast-marching level set approach for segmenting the breast in mammography images where the initial breast region is segmented by thresholding the image and keeping the object with the highest number of connected pixels. The final breast boundary is then approximated using a level set method and refined using sequentially alternating morphological filters. Evaluated on a subset of 100 images from the mini-MIAS dataset, their proposed method was able to achieve an average sensitivity and precision of 98.6% and 99.1%, respectively.

4.3 Clustering based methods

Clustering based segmentation methods are based on the assumption that pixels belonging to certain objects can be clustered together using a single or a set of predefined properties such as a certain intensity range, adjacency and texture, to name a few. Clustering methods can be implemented using either a supervised or an unsupervised approach with the unsupervised approach being the most popular clustering approach for the breast segmentation in mammography images (with K-means being the most popular method). In most of the unsupervised clustering approaches, the number of the predefined clusters (must be defined prior to the segmentation) can affect the accuracy of the segmentation to a large degree. Recent clustering methods are often combined with evolutionary computing-based optimization techniques such as genetic algorithm and cuckoo optimization for enhancing their accuracy.

Rickard et al. (2004) proposed breast segmentation method using a multi-scale analysis approach where the images are filtered utilizing Gaussian filters with different standard deviations convolved with combinations of the derivative of a Gaussian function for identifying different clusters of objects in the image with similar intensities. Evaluated on a subset of 400 images from the DDSM dataset (containing both the MLO and CC projections), their proposed method was able to achieve varying accuracy based on overall image density and the number of predefined clusters using visual inspection of the accuracy of the segmentation without using any statistical performance measures. The process of pre-defining the num-

ber of clusters is one of the main drawbacks associated with their proposed method as the quality of segmentation is highly dependent on the number of clusters defined. Slavković-Ilić et al. (2016) proposed using a K-means clustering algorithm for segmenting the breast tissue in mammograms with the contrast of the image enhanced using the Adaptive Gamma Correction with Weighting Distribution (AGCWD) method (Huang et al. 2013). K-means algorithm is used for detecting the initial breast boundary and the cluster with the lowest mean intensity is taken as the background. Mathematical morphology is then used to remove any artifacts such as labels and the breast boundary is smoothed using a large 20×20 averaging filter. Evaluated on the mini-MIAS dataset using visual inspection of the accuracy of the segmentation, their proposed method was able to provide good and acceptable segmentation in 90.68% and 6.83% of the cases, respectively. Sampaio et al. (2011) also proposed using the K-means clustering algorithm for segmenting the breast region in mammograms. The image is segmented using a K-means algorithm with two clusters and the cluster with the lowest mean intensity is taken as the background with the pixels correlating to the background cluster being removed from the image. The boundaries of remaining regions are then refined using a region growing method and the object with the highest number of connected pixels is taken as the breast region. Nazaré et al. (2015) also proposed a similar approach for segmenting the breast tissue in mammograms with a 3×3 median filtering of the images (for noise reduction) prior to the K-means clustering being the main difference between their proposed method and the method proposed by Sampaio et al. (2011). Both methods were validated using visual inspection of the accuracy of the segmentation without providing any detailed statistical performance measures. Yoon et al. (2016) also proposed using a k-means algorithm for segmenting the breast region in mammography images. Similar to the method proposed by Sampaio et al. (2011), the image is segmented using a K-means algorithm with two clusters and the cluster with the lowest mean intensity is taken as the background with the pixels correlating to the background cluster being removed from the image with mathematical morphology beings used for smoothening the segmented breast boundary. Evaluated using the mini-MIAS dataset based on visual inspection of the accuracy of the segmentation, their proposed method was able to provide good and acceptable segmentation in 81.98% and 11.18% of the images, respectively.

4.4 Region growing and graph-cut based methods

Region-based segmentation methods work on the assumption that pixels belonging to certain objects will have similar properties (such as a certain intensity range) with region growing and watershed techniques being the most popular approaches. In region growing techniques, a seed pixel (or a set of seed pixels in more recent methods) are defined inside the region of interest and the adjacent pixels to these seed points are added to the ROI based on a predefined merging criterion such a similar intensity. Often, region growing methods will ignore weak edges in the image (although this attribute can result in over segmentation in images where most of the edges are weak) and stop at locations with strong edges (such as the boundary between the breast and background) based on the merging/stopping criterion set. Although region growing methods are often accurate, defining the initial seed(s) can be difficult with the final segmentation accuracy being highly dependent on the initial seed(s). As a result, most region growing methods use other segmentation/localization approaches for estimating an initial ROI candidate for the seed placement or require the user to provide the initial seed(s). Graph Cut (GC) segmentation (a variation of region growing) has been gaining popularity in medical image segmentation tasks where the image pixels are represented as nodes on

a graph with the adjacency between the pixels being represented as weighted edges on the graph where the image is segmented by computing the minimum cost function amongst all possible cuts of the graph. Similar to region-based segmentation methods, the GC method requires a set of pixels to be defined as belonging to the background and the ROI.

Zhang et al. (2010) proposed a method for breast boundary segmentation where the image is enhanced utilizing low-pass filtering with the initial breast region estimated by thresholding and keeping the object with the highest number of connected pixels. Finally, the breast is segmented using a region growing approach with seeds located inside the estimated breast region and the background positioned using approximate endpoints of a line connecting the top-left corner of the image to the low-right corner of the image. Evaluated on a subset of 20 images from the mini-MIAS dataset, their proposed method was claimed to have good performance based on a visual inspection of the accuracy of the segmentation without providing any detailed statistical performance measures. The main drawback of their proposed approach is the placement of the region growing seeds as the seed locations chosen are dataset dependent and might not work correctly if applied to other datasets (especially larger datasets). Saidin et al. (2010) proposed a semi-automatic breast segmentation approach using a GC method where the user is required to manually assign seeds representing the breast and the background regions. Although their proposed method can achieve good accuracy in most images, the amount of manual interactions required makes this approach not suitable for clinical and/or everyday use.

Wei et al. (2006) proposed using a global thresholding approach coupled with morphological operations for estimating the initial breast boundary and removing background objects such as labels. The breast boundary is then refined by a watershed transform based on a combination of region growing and edge detection techniques. Their proposed method was shown to achieve good performance based on a visual inspection of the accuracy of the segmentation with an average of 94.9% images from DDSM dataset being segmented with acceptable accuracy. Raba et al. (2005) proposed a method for breast boundary segmentation where the initial breast boundary is estimated using a set of different thresholds applied to different patches inside the image. Then, the mean intensity value inside a set of overlapping breast patches segmented by the lowest threshold and the highest threshold is computed. Finally, the initial breast region is localized using the computed mean intensity with the breast boundary refined using a selective region growing approach. Evaluated using the MIAS dataset with reduced spatial dimensions (for faster processing), their proposed method was able to achieve an average segmentation accuracy of 98%.

4.5 Other methods

Apart from the mentioned methods, there are some other successful methods for segmenting the breast region, often combining several image segmentation methods together. Karnan and Thangavel (2007) proposed using a genetic algorithm based clustering approach for segmenting the breast region in mammograms. First, an initial breast boundary is approximated using a thresholding approach with morphological operations used for removing background objects and noise such as labels. Then, a genetic algorithm based clustering approach is used for refining the breasts region based on the approximated breast boundary. While images from the MIAS dataset were used in their study, they validated their results using visual inspection of the accuracy of the segmentation without providing any detailed statistical performance measures. Wirth et al. (2004) proposed a pixel-wise fuzzy breast region segmentation approach based on a fuzzy combination of the deviation magnitude and

the sharpness measure of the edges in a neighboring window of the pixel being processed for identification of boundary pixels. Evaluated on a subset of 120 images from the MIAS dataset, their proposed method was able to achieve a mean sensitivity of 99% and precision of 98%.

Chen and Zwiggelaar (2012) proposed a multistep method for extracting the breast boundary. The initial breast region is segmented using thresholding by considering the middle-intensity value between the two largest peaks in the image histogram as the threshold value followed by morphological operations for removing small background objects such as labels and taking the object with the highest number of connected pixels as the initial breast boundary. This boundary is then refined by placing 40 points along the boundary and performing edge detection on a 100 pixels wide orthogonal line (to the breast boundary) at each of the 40 points with this process being repeated 3 times using a Gaussian kernel with different scales. Finally, the breast boundary is determined by a cubic polynomial fitting method applied to seed points computed using a contour growing method utilizing one seed point per each orthogonal line (40 seeds in total). Evaluated using the MIAS dataset, their proposed method was able to achieve an accuracy of 98.8%. Casti et al. (2013) proposed using Otsu's thresholding method coupled with a Gabor filtering technique for extracting the breast boundary. The breast region is approximated by thresholding the image using the Otsu's thresholding method and then the Euclidean distance transform (EDT) of the resulting binary image is computed. The edges are enhanced using adaptive values-of-interest (VOI) transformation and edge responses from 18 different Gabor filters are computed and imposed on top of each other with responses not lining up with the approximate breast boundary being discarded. Finally, edges are linked together and the final breast boundary is extracted. Evaluated using 249 mammograms from the mini-MIAS dataset and 194 FFDM images from a private dataset, their proposed method was able to achieve an average sensitivity and precision of 99.8% and 99.5%, respectively.

Based on the notion of artifacts having straight lines as their boundaries (such as labels), Torres and Pertuz (2017) proposed a statistical approach for extracting the artifacts in mammography images. The initial breast boundary is detected using a statistical approach by treating pixels belonging to the breast as samples from a normal distribution based on Anderson–Darling test (Liu et al. 2011) based on the notion that the breast tissue pixels have some texture while the background is mostly homogenous. Utilizing an empirically determined p value, initial breast boundary is segmented by assigning pixels over the determined p -value to the breast region with this boundary refined using mathematical morphology. Evaluated on the DDSM dataset, their proposed method was able to provide correct segmentation in 32.28% of the cases. Tzikopoulos et al. (2009) proposed using polynomial fitting for extracting the breast boundaries (polynomial fitting is more popular in pectoral muscle segmentation). The images used in their study were transformed as to have the chest wall on the left side of the image. Then, small background objects such as labels are removed using thresholding combined with morphological operations. Based on the notion of the skin-air interface surrounding the breast having the smoothest variations in intensity, polynomial fitting with orders of 5 to 10 were applied to the initial breast boundary with different threshold values. Finally, the breast is segmented by taking the polynomial fit with the least error as the boundary. While computationally demanding, their proposed method was able to achieve a DSC of 0.945 evaluated using the mini-MIAS dataset.

Gradient-based approaches can also be used for segmenting the breast boundary as they can detect gradient magnitude changes occurring due to a large intensity discrepancy in the boundary of different objects (compared to the background) in the mammograms. Shi et al. (2018) proposed using a gradient-based method for extracting the breast boundary.

First, a weight is assigned to each pixel by combining the gradient of adjacent pixels on the horizontal and vertical axis using a 3×3 sliding window. Then, the gradient image is cleaned using morphological eroding and the breast region is segmented by taking the object with the highest number of connected pixels. Finally, the boundary is refined by removing the area where there is a sharp change in the curvature of the breast boundary by a horizontal line at the top inflection point using a 2D curvilinear structure localization. Evaluated using the MIAS dataset, their proposed method was able to achieve an average accuracy of 97.08%.

4.6 Summary

The quality of the mammography images can be considered as the main factor influencing the accuracy of different breast boundary segmentation methods. As a result, many methods have validated their approach using a subset of images from various datasets and not the entire dataset (with MIAS and mini-MIAS datasets being more popular as they have higher quality images compared to DDSM dataset). As there is no gold standard for many of the breast boundary segmentation datasets apart from the MIAS dataset (although many datasets have the gold standard segmentations for the masses), most methods use the manual segmentation by different users/experts as the gold standard in their study or base the accuracy on a visual inspection of correctness of the segmentation, making a direct comparison between the performance of these methods difficult. However, based on the literature, many of the proposed methods can be considered as an effective breast boundary segmentation approach. Moreover, the use of intensity-based thresholding and mathematical morphology can be considered as the basis for most breast boundary segmentation methods. In mammography images, breasts can be segmented with simpler image segmentation concepts as the difference in intensity and the shape between the breasts and the background is high. Currently, labels that are positioned too close to the breast boundary can be considered as the main difficulty for achieving a satisfactory segmentation in all datasets. However, with FFDM imaging becoming more popular and accessible, breast boundary segmentation will become more accurate as the labels and markings can be removed from the original DICOM images with ease (coupled with the higher quality of FFDM images). Table 2 shows a comparison between different breast region segmentation methods.

5 Segmentation of pectoral muscle from MLO mammograms

As some parts of the pectoral muscle are also imaged during the mammogram acquisition using the MLO plane, it is desired to remove this muscle for simplifying the abnormality detection and increasing the accuracy of CAD as both fibroglandular tissues and pectoral muscle tissues are considered to have similar image characteristics. Pectoral muscle, often seen near the chest wall approximately on the upper region of the mammogram, appears as a bright region as it is denser than the breast tissue (due to higher absorption of X-rays) as illustrated in Fig. 11. This difference in attenuation, while not always well defined, is the basis of most pectoral muscle segmentation approaches.

Although many pectoral muscle segmentation methods often include a breast boundary segmentation step, it is possible to segment the pectoral muscle without segmenting the breasts. Additionally, while some methods rely on the expected location of the pectoral muscle for their segmentation, these methods can have difficulties in cases where the image is not aligned correctly or in cases where the pectoral muscle is not contained within this

Table 2 Comparison between different breast region segmentation methods

Proposed by	Method used	Method complexity	Dataset (subset of images used)	Accuracy	Other performance measures
Mustra and Grgic (2013)	Thresholding	Medium	mini-MIAS	99.1%	96.3% VO
Qayyum and Basit (2016)	Thresholding	Low	mini-MIAS	99.37% (visual validation)	Not mentioned
Maitra et al. (2012)	Thresholding	Low	mini-MIAS	95.7%	Not mentioned
Mustra et al. (2009)	Thresholding	Low	FFDM	100%	Not mentioned
Wirth and Stapinski (2003), semi-automatic	Active contours	Low	MIAS (25)	Not mentioned	97% VO
Rampun et al. (2017)	Active contours	High	MIAS	98.4%	0.988 DSC
Martí et al. (2007)	Active contours	High	MIAS (65) DDSM (24)	Not mentioned	96% sensitivity 96% precision
Ferrari et al. (2004a)	Active contours	Medium	mini-MIAS (84)	Not mentioned	0.41% FP 0.58% FN
Yapa and Harada (2008)	Level set	Medium	mini-MIAS (100)	Not mentioned	98.6% sensitivity 99.1% precision
Slavković-Ilić et al. (2016)	K-means clustering	Medium	mini-MIAS	97.51% (visual validation)	Not mentioned
Yoon et al. (2016)	K-means clustering	Low	mini-MIAS	93.16% (visual validation)	Not mentioned
Wei et al. (2006)	Region growing	Medium	DDSM	94.9% (visual validation)	Not mentioned
Raba et al. (2005)	Region growing	Medium	MIAS	98%	Not mentioned
Wirth et al. (2004)	Fuzzy rule based segmentation	High	MIAS (120)	Not mentioned	99% sensitivity 98% precision
Chen and Zwiggelaar (2012)	Polynomial curve fitting	High	MIAS	98.8%	Not mentioned
Casti et al. (2013)	Edge detection using Gabor filters	Medium	mini-MIAS (249) FFDM (194)	Not mentioned	99.8% sensitivity 99.5% precision
Torres and Pertuz (2017)	Statistical region properties	Medium	DDSM	32.28%	Not mentioned
Tzikopoulos et al. (2009)	Polynomial curve fitting	High	mini-MIAS	Not mentioned	0.945 DSC
Shi et al. (2018)	Gradient based thresholding	Low	MIAS	97.08%	Not mentioned

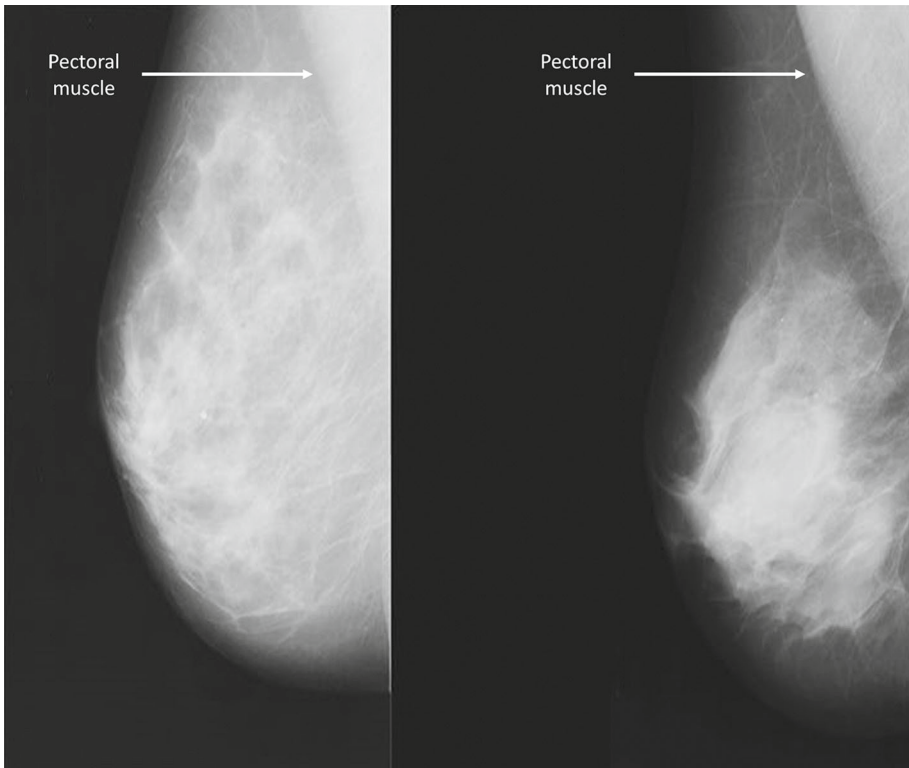


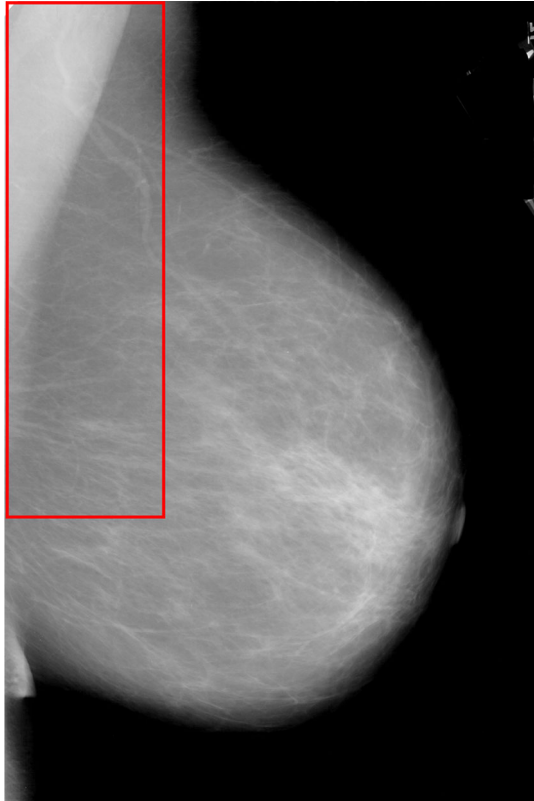
Fig. 11 Sample images illustrating the difference in attenuation between the breast and pectoral muscle regions

expected region. Many of the pectoral muscle segmentation methods will try to locate the pectoral muscle within a predefined (although varying) region of interest (ROI) near the chest wall as illustrated in Fig. 12. Often, the pectoral muscle location (left or right of the mammogram) is found by considering a line dividing the mammogram (image) at half of its length and then computing the number of foreground pixels (or the sum of pixel intensities in some methods) for each half. The half containing the highest number of pixels (or the sum of intensity) is then taken to be containing the pectoral muscle and the image can be then transformed (if needed) to have the pectoral muscle in the left region of the image.

5.1 Thresholding and intensity-based methods

Unlike breast segmentation where the intensity can be effectively used for separating the breast and the background, sole use of intensity for segmenting the pectoral muscle from the breast region cannot produce accurate segmentation in most cases. This can be contributed to the inconsistent and often non-significant intensity variation between the pectoral muscle tissue and other tissues in the breast. Based on the assumption that the pectoral muscle is expected to be located in the left region of the image near the chest wall, Subashini et al. (2010) proposed a thresholding approach for removing the pectoral muscle from a pre-segmented breast region. They used a simple thresholding approach without any refinement steps for segmenting the pectoral muscle boundary with no statistical performance measures provided.

Fig. 12 The predefined ROI often used for the pectoral muscle segmentation represented as the red rectangle



Tayel and Mohsen (2010) proposed an intensity-based approach for removing the pectoral muscle from a pre-segmented breast region where the pectoral muscle is located by comparing the intensities between the upper-left region of the image and the rest of the breast as it was assumed that the pectoral muscle pixels will have a higher intensity compared to the breast tissue with no detailed statistical performance measures provided. Czaplicka and Włodarczyk (2012) proposed using iterative thresholding for approximating the initial pectoral muscle boundary followed by a linear regression method for refining the boundary. However, they did not provide much information on their proposed methodology. They validated their results on the mini-MIAS dataset claiming that 98% of the images were segmented accurately based on a visual inspection of the accuracy of the segmentation without providing any detailed statistical performance measures.

Shrivastava et al. (2017) proposed a sliding window-based approach for removing the pectoral muscle from mammograms. The mammogram images are converted to 8-bits and transformed so that the chest wall would be positioned on the left side of the image (as their proposed method requires the pectoral muscle to be located in the upper-left region of the image, near the chest wall). Then, a 5×5 window is defined on the top-left corner of the image and the total intensity inside the window and the absolute intensity difference between the top left and bottom right pixels inside the window are computed. The window then slides through the image (in a distinct manner) and is considered to contain a pectoral muscle segment as long as the total window intensity remains over a pre-set threshold of 3000 and absolute intensity difference between the top left and bottom right pixels inside the

window remain under 250. Their proposed method was able to successfully segment 91.3% of images based on visual inspection of the accuracy of the segmentation using the MIAS dataset without providing any detailed statistical performance measures. Sreedevi and Sherly (2015) proposed using a global threshold for estimating the initial pectoral muscle boundary followed by morphology-based boundary refinement. The original images are normalized for enhancing the contrast and transformed so that the chest wall would be positioned on the left side of the image. Initial pectoral muscle region is then segmented using a combination of global thresholding and connected components with this boundary being refined using mathematical morphology. Validated using a subset of 161 images from the mini-MIAS dataset, it was claimed that 90.06% of the images were segmented accurately based on visual inspection of the accuracy of the segmentation without providing any detailed statistical performance measures. Unni et al. (2018) proposed using a global threshold for estimating the initial pectoral muscle boundary followed by morphological methods for refining the boundary, similar to the method proposed by (Sreedevi and Sherly 2015). The original images are transformed so that the chest wall would be positioned on the left side of the image. The Initial pectoral muscle region is then segmented using a combination of global thresholding (with a threshold value of 160) and connected components with this boundary being refined using mathematical morphology. They validated their method using visual inspection of the accuracy of the segmentation without providing any detailed statistical performance measures.

5.2 Region growing methods

The region growing approach proposed by Chen and Zwigelaar (2012) begins by approximating the pectoral muscle boundary using the intensity variations inside the image. Then, seeds for the region growing method are placed near this initial boundary and the pectoral muscle is segmented and then refined using a locally weighted scatter-plot smoothing function. Evaluated using the mini-MIAS dataset, their proposed method was able to produce 67.9% accurate, 24.9% nearly accurate and 5% acceptable segmentations that totals in 97.8% of the images having an acceptable segmentation. Ergin et al. (2016) proposed a region growing based approach for removing the pectoral muscle from a pre-segmented breast outline where the image noise is reduced using median filtering. The position of initial seeds for the pectoral muscle region is then determined based on the region intensity followed by the region growing method for determining the final muscle boundary. They validated their results using visual inspection of the accuracy of the segmentation without providing any detailed statistical performance measures.

Nagi et al. (2010) also proposed using a region growing approach for pectoral muscle segmentation from a pre-segmented breast region based on the assumption that the pectoral muscle is expected to be located near the chest wall approximately on the upper-left region of the image. Based on the assumed pectoral muscle location and intensity, seeds for region growing algorithm are defined and the image is segmented. Interestingly, although region growing is capable of segmenting a curved boundary, Nagi et al. (2010) used a straight-line approximation of the boundary segmented by the region growing for segmenting the pectoral muscle. As a result, their method was not deemed to provide acceptable segmentation in all images based on a visual inspection of the accuracy of the segmentation without using any detailed statistical performance measures. A similar approach based on the assumed position of the pectoral muscle was proposed by Maitra et al. (2012) whereas by taking the boundary of the pectoral muscle as a curved line instead of the straight-line approach used by Nagi

et al. (2010), their proposed method was able to segment 95.65% of images from the mini-MIAS dataset with acceptable accuracy. Esener et al. (2018) also proposed using a region growing approach for pectoral muscle segmentation from a pre-segmented breast region based on the assumption that the pectoral muscle is expected to be located near the chest wall approximately on the upper-left region of the image. Based on the assumed pectoral muscle location and intensity, a single seed for region growing algorithm is defined and the image is segmented. Interestingly, although region growing is capable of segmenting a curved boundary, Esener et al. (2018) also used a straight-line approximation of the boundary determined by the region growing for segmenting the pectoral muscle. As a consequence, their method could result in under-segmentation of the pectoral muscle boundary as their proposed method was able to achieve an accuracy of 94.4%, a sensitivity of 89.62% and specificity of 99.99%, evaluated using the MIAS dataset.

Raba et al. (2005) also proposed a region growing based approach for removing the pectoral muscle from a pre-segmented breast outline. To limit the possibility of over-segmentation, Raba et al. (2005) used a pre-set threshold for the number of segmented pectoral muscle pixels with the final boundary refined using mathematical morphology. Evaluated using the mini-MIAS dataset, their proposed method was able to achieve an acceptable accuracy in 86% of images according to a visual inspection of the quality of segmentation. Saltanat et al. (2010) proposed a region growing approach for pectoral muscle segmentation based on the assumption that the pectoral muscle is expected to be located near the chest wall approximately on the left-upper region of the mammogram. The contrast of the image is enhanced and the boundaries between different tissues are sharpened using grayscale-based morphology operations (opening and closing). Finally, based on the assumed pectoral muscle location, seeds for a region growing method are defined and the pectoral muscle is segmented. Evaluated using the mini-MIAS dataset, their proposed method was able to achieve an acceptable accuracy in 84% of images according to the first radiologist checking the results and 92% of images according to a second radiologist. A region growing approach governed by a set of geometric rules for removing the pectoral muscle from a pre-segmented breast region was proposed by Taghanaki et al. (2017) based on the fact that the intensity cannot be used effectively for detecting complex textures such as the muscles. In their proposed method, the image intensity is rescaled to a range from 0 to 1 and the contrast between different tissue types in the image is enhanced using the CLAHE technique with the image then being converted to binary using a threshold of 0.03 (a threshold of approximately 8 in case of 8-bit images). The initial pectoral muscle region is then defined based on a set of geometric rules and refined using a region growing method. Evaluated using the MIAS and DDSM datasets, their method was able to provide acceptable segmentation in 95% and 94% of the images, respectively.

Based on the assumption that the pectoral muscle is expected to be located in the upper region of the image near the chest wall, Camilus et al. (2010) proposed a graph-cut approach for removing the pectoral muscle from mammograms. Initial pectoral muscle region is approximated using thresholding (for determining the seed points) and graph-cut segmentation methods with the final refined boundary computed by a Bezier curve fitting approach. Their proposed method was able to achieve a FP rate of 0.64% and a FN rate of 5.58% evaluated using a subset of 84 random images from the mini-MIAS dataset. Camilus et al. (2011) later improved this approach by replacing the graph-cut method with watershed segmentation. A curve estimation method is used for refining the initial pectoral muscle boundary segmented using the watershed method with their improved method achieving in an acceptable segmentation in 94% of images evaluated using the same 84 images from the mini-MIAS dataset. A similar approach based on graph-cut and Bezier curve estimation was also pro-

posed by Abdellatif et al. (2019) with their method achieving a FP rate of 1.2% and a FN rate of 20.4%, evaluated using a subset of 80 random images from the mini-MIAS dataset.

Selvathi and Poornila (2018) proposed using a region growing approach for pectoral muscle segmentation from a pre-segmented breast region based on the assumption that the pectoral muscle is expected to be located near the chest wall approximately on the upper-left or upper-right region of the image. Based on the assumed pectoral muscle location, a single seed for region growing algorithm is defined and the image is segmented. Interestingly, while most methods incorporate an additional step (often intensity based) for identifying the optimal location(s) of seed point(s), their proposed method will take the pixel at the 5th column of the 5th row as the seed for the region growing in images where pectoral muscle is positioned on the left of the image and the last 5th column in images where pectoral muscle is positioned on the right. The pectoral muscle boundary is then refined using morphology-based filtering operations utilizing a disc structuring element with a radius of 5 pixels. They validated their results using visual inspection of the accuracy of the segmentation without providing any detailed statistical performance measures. Hazarika and Mahanta (2018) also proposed a similar approach based on the assumed position of the pectoral muscle where a gradient-based smoothing method is used for refining the segmented pectoral muscle boundary (instead of morphology-based filtering). Validated using a subset of 150 images from the mini-MIAS dataset, their proposed method was able to achieve acceptable and partially acceptable segmentation in 86.67% and 5.33% of the images, respectively. Saidin et al. (2010) proposed a semi-automatic pectoral muscle segmentation using graph-cut method. Their proposed method is time-consuming as the user is required to provide the initial seeds for the pectoral muscle region with the final segmentation being dependent on this initial placement of seeds. They validated their results using visual inspection of the accuracy of the segmentation without providing any detailed statistical performance measures.

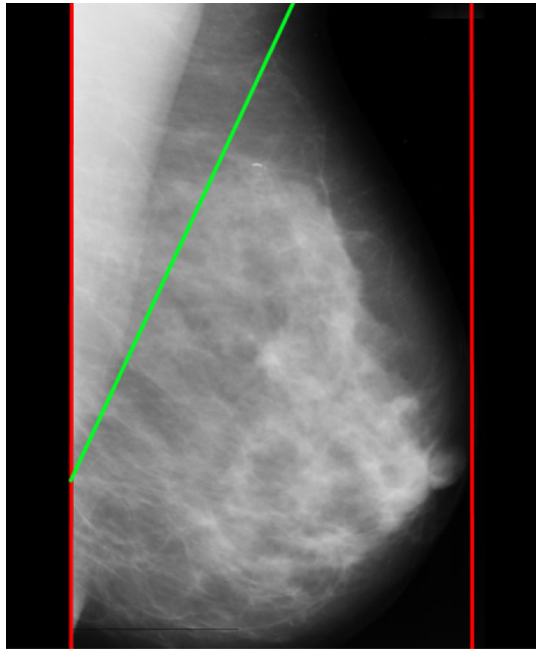
5.3 Line estimation methods

Line estimation methods can be considered as one of the most popular pectoral muscle segmentation approaches and are based on the notion that the pectoral muscle boundary can be represented by a curved or a straight line. Hough transform (Ballard 1987) can be considered as the most popular line estimation method used for pectoral muscle segmentation that can be used for estimating both straight and curved lines. Based on the assumption that the pectoral muscle is expected to be located in the upper region of the image near the chest wall, Weidong and Shunren (2003) proposed a line estimation method for removing the pectoral muscle from mammograms. The expected region of interest (taken as a quarter of the image) is defined based on the orientation of the image and the initial pectoral muscle region is segmented using an iterative thresholding method. To compensate for possible variations in the pectoral muscle size, different window sizes are used to threshold the candidate region and the window with the largest number of segmented pectoral muscle pixels (based on the higher attenuation) is chosen. Finally, the pectoral muscle outline is estimated and extracted using the Hough transform and polygonal modeling methods. Evaluated using an unspecified dataset containing 60 images, their proposed method was able to achieve an acceptable segmentation in 81.7% of images based on visual inspection of the accuracy of the segmentation. Ferrari et al. (2004b) proposed a Hough transform based approach for removing the pectoral muscle from mammograms. Although Hough transform can be used to find any arbitrary shapes (used mostly for finding circles and curved lines), Ferrari et al. (2004b) used Hough transform for finding a straight line that best estimates the true pectoral muscle boundary. As a straight

line cannot adequately represent a curved boundary, the accuracy of their method was not high with a FP rate of $1.98 \pm 6.09\%$ and a FN rate of $25.19 \pm 19.14\%$, evaluated using a subset of 84 images from the mini-MIAS dataset. Ferrari et al. (2004b) also proposed using Gabor filters for approximating the pectoral muscle boundary by locating pixels that have the opposite phase orientation. While more accurate, selecting the correct boundary computed from different scales of the Gabor filters can be a challenging task. The proposed Gabor based approach was able to achieve a FP rate of $0.58 \pm 4.11\%$ and a FN rate of $5.77 \pm 4.83\%$, evaluated using the same subset of 84 images from the mini-MIAS dataset. Sampaio et al. (2011) proposed a Hough transform based approach for removing the pectoral muscle from a pre-segmented breast region with the contrast of the images enhanced using histogram equalization. In their proposed method, the initial pectoral muscle location is found by considering a line dividing the mammogram picture at half its width and then computing the mean intensity for each half. The half with the highest mean intensity is then taken to be containing the pectoral muscle with a straight-line estimating the true pectoral muscle boundary computed using Hough transform. They validated their results using the DDSM dataset based on visual inspection of the accuracy of the segmentation without providing any detailed statistical performance measures.

A hybrid pectoral muscle removal approach combining adaptive thresholding with a Hough transform for removing was proposed by Xu et al. (2007). The initial segmentation of the pectoral muscle region was done using an adaptive thresholding approach and Hough transform. Finally, the pectoral muscle boundary was refined with an elastic thread technique. Evaluated using a private dataset of 52 images, their proposed method was able to achieve an acceptable VO of 94.5%. Qayyum and Basit (2016) proposed using a Canny edge detector for removing the pectoral muscle region from mammograms with a 3×3 median filter being used for reducing the noise in the mammogram image. The initial pectoral muscle region is estimated based on a combination of Canny edge detector (Canny 1986) and the region intensity with the final pectoral muscle boundary determined using a straight-line estimation method applied to the boundary candidate. Evaluated using the mini-MIAS dataset based on visual inspection of the accuracy of the segmentation, their proposed method was able to provide acceptable segmentation in 93% of the cases. Zhou et al. (2017) and Xie et al. (2016a, b) both proposed using a straight-line estimation method based on Linear Hough Transform for segmenting the pectoral muscle boundary. Initial pectoral muscle boundaries were approximated using a Sobel operator configured for detecting horizontal edges followed by Linear Hough Transform for determining the pectoral muscle boundary. They both validated their results using visual inspection of the accuracy of the segmentation without providing any detailed statistical performance measures. Based on the assumption that the pectoral muscle is expected to be located in the upper-left region of the image near the chest wall, Palkar and Agrawal (2016) proposed a straight-line estimation approach for removing the pectoral muscle from mammograms. The original images were transformed so that the chest wall would be positioned on the left side of the image. Then, the middle-top pixel of the image is connected to the lowest-left pixel of the rectangle approximating the pectoral muscle with the straight-line connecting these pixels taken as the pectoral muscle boundary. Finally, the image is segmented based on segmented breast and pectoral muscle boundaries as illustrated in Fig. 13. They validated their results based on a visual inspection of the accuracy of the segmentation using the MIAS dataset where the segmentation was claimed to be successful in 80% of images. A similar straight-line estimation approach for removing the pectoral muscle from mammograms was also proposed by Sasikala and Ezhilarasi (2018) where they too validated their results based on a visual inspection of the accuracy of the segmentation without providing any detailed statistical performance measures.

Fig. 13 Straight-line estimation approach for pectoral muscle segmentation proposed by Palkar and Agrawal (2016) with red lines representing the breast region and the green line representing the pectoral muscle boundary. (Color figure online)



5.4 Curve estimation methods

Shi et al. (2018) proposed an approach for removing the pectoral muscle from mammograms using a four-class K-means clustering method based on the assumption that the pectoral muscle is expected to be located near the chest wall approximately on the left-upper region of the mammogram. First, the noise in the images is reduced using a 5×5 median filter and the images are normalized for enhancing the contrast. Then, the pixels are clustered using K-means clustering and the cluster with the highest intensity is taken as the potential pectoral muscle region candidate based on the expected pectoral muscle location with clusters containing less than 100 pixels being removed. The cluster boundary is then smoothed using morphology operations and a Hough transform method is used for extracting the initial pectoral muscle boundary. The final boundary is then refined by a polynomial curve fitting method using a second-degree polynomial (Lancaster and Salkauskas 1986). Evaluated using the MIAS dataset, their method was claimed to provide acceptable segmentation in most of the images without providing any detailed statistical performance measures.

Mustra and Grgic (2013) proposed an approach for removing the pectoral muscle from mammograms using a polynomial fitting method. Images are first enhanced using the CLAHE method and then the initial pectoral muscle region is determined using thresholding with 10 points along the boundary chosen for the polynomial fitting based on the assumption that the pectoral muscle is expected to be located near the chest wall approximately on the left-upper region of the mammogram with the boundary refined by a polynomial fitting method using a third-degree polynomial. Evaluated using the mini-MIAS dataset, their method was able to provide acceptable segmentation in 96.6% of the images. Shen et al. (2018) proposed a multilevel thresholding approach for removing the pectoral muscle from the segmented breast where the tissues inside the breast are clustered using multiple thresholds computed by a genetic algorithm based clustering approach (Hammouche et al. 2008). An initial pectoral

muscle region is determined using a morphological selection algorithm based on the assumption that the pectoral muscle region could be (roughly) represented as a triangle with high overall intensity with a gradual reduction in the width when measured from top to bottom. The final pectoral muscle boundary is then determined by refining the initial boundary using a cubic polynomial fitting approach. Evaluated on the mini-MIAS dataset and a subset of 128 low-contrast images from the DDSM dataset, their proposed method was able to achieve a DSC of 0.9496 and 0.9715, respectively. Additionally, their method was also able to segment the pectoral muscle with acceptable accuracy in 96.81% of images from the mini-MIAS dataset.

5.5 Cliff detection methods

Kwok et al. (2004) proposed using Hough transform for detecting the strongest straight line representing the pectoral muscle boundary with cliff detection carried along the entire line to compensate for variations in the size and the shape of the pectoral muscle. Evaluated using the MIAS dataset (down-sampled for faster processing), their proposed method was able to achieve an acceptable accuracy in 88.8% of images according to the first radiologist checking the results and 80.1% of images according to a second radiologist. Using cliff detection for pectoral muscle segmentation was also proposed by (Tzikopoulos et al. 2009) with a straight-line detection method being used for approximating the initial pectoral muscle boundary followed by Iterative cliff detection for refining this initial boundary. They validated their results on the mini-MIAS dataset using visual inspection of the accuracy of the segmentation without providing any detailed statistical performance measures. Based on the notion that the pectoral muscle is expected to be located near the chest wall approximately on the upper region of the mammogram, Kwok et al. (2001) proposed an iterative thresholding method for detecting the approximate outline of the pectoral muscle coupled with cliff detection along an estimated straight line (as the pectoral muscle boundary). The pectoral muscle region is first filtered using a bi-cubic spline interpolation followed by edge detection for extracting the initial pectoral muscle boundary and refined using morphological closing. Evaluated utilizing the MIAS dataset, their proposed method was able to achieve an acceptable accuracy in 94% of images based on visual inspection of the accuracy of the segmentation. The method proposed by Kwok et al. (2001) was later used by Nayak et al. (2019) where the images are filtered using morphological Top-hat filtering prior to pectoral muscle boundary detection. Evaluated using the MIAS dataset, their method was claimed to provide acceptable segmentation in most of the images without providing any detailed statistical performance measures.

5.6 Other methods

Apart from the mentioned methods, there are some other successful methods for segmenting the pectoral muscle region, often combining several image segmentation methods together. Based on the assumption that the pectoral muscle is expected to be located in the upper-left region of the image near the chest wall, Li et al. (2013) proposed an approach for removing the pectoral muscle from mammograms using texture analysis. Based on the notion that the intensity varies a lot near the pectoral muscle boundary, two likelihood maps are computed using the intensity and texture fields. Then, these maps are combined and the maxima points are taken as an initial representation of the pectoral muscle region. Finally, the approximated initial boundary is refined using a Kalman filter (incorporating the spatial distance of pixels). Their method was able to provide acceptable segmentation in 90% of the images from the

mini-MIAS dataset and 92% using a subset of 100 images from the DDSM dataset. A pectoral muscle segmentation method using an average gradient with a shape-based feature was proposed by Chakraborty et al. (2012). Their proposed method starts by approximating a straight line representing the pectoral muscle boundary with the final boundary extracted and smoothed using an average gradient with a shape-based feature. Evaluated using 80 images from the mini-MIAS dataset and 80 FFDM images from a private dataset, their proposed method achieved an average VO of 89.08% and 89.25%, respectively. Sultana et al. (2010) proposed a mean-shift clustering approach with a Gaussian kernel for differentiating various tissues inside the mammogram using a pixel neighbor connectivity for segmenting tissues with similar spatial characteristics. Their proposed method was able to achieve a TP rate of 84% and a FP rate of 13%, evaluated using the mini-MIAS dataset. Ma et al. (2007) proposed an active contour-based approach for pectoral muscle segmentation using the notion that the pectoral muscle is expected to be located near the chest wall, approximately on the left-upper region of the mammogram. Initial pectoral muscle boundary is computed by taking multiple possible edge candidates based on changes in the intensity near the boundary. Then, the strongest edge candidate is selected by a minimum spanning trees method and used in the initialization of an active contour-based approach for refining the final boundary. Ma et al. (2007) also proposed a graph-cut based approach for pectoral muscle segmentation based on seeds positioned according to the strongest edge candidate with the results achieved by the graph-cut based approach being superior to the active contour approach. The graph-cut based approach was able to achieve a FP rate of $0.58 \pm 4.11\%$ and a FN rate of $5.77 \pm 4.83\%$, evaluated using a subset of 84 images from the mini-MIAS dataset.

Adel et al. (2007) proposed using Markov random fields and Bayesian segmentation for differentiating various tissues inside the mammogram using a pixel-wise, 8-nearest-neighbor connectivity measure for clustering tissues with similar intensities. While an interesting approach, their method had considerable difficulty in achieving good accuracy (due to the amount of noise and various anatomical structures inside the breast). Evaluated using an unspecified dataset containing 50 images, their proposed method was able to achieve an acceptable accuracy in 68% of images according to a visual inspection of the quality of segmentation. Using Markov random fields for pectoral muscle segmentation was also proposed by Wang et al. (2010). Their method creates a matrix of pixel values by scanning each row of the image pixels based on the assumption that the difference in intensity between the pectoral muscle and the rest of the breast tissue would be high with points having the highest standard deviation being considered as the initial pectoral muscle boundary. Finally, the boundary is refined using an active contour approach. Evaluated on a subset of 200 images from the DDSM dataset, their proposed method was able to achieve an acceptable accuracy in 84% of images without active contour refinement and 91% with refinement according to a visual inspection of the quality of segmentation. Mustra et al. (2009) proposed a wavelet-based decomposition approach for removing the pectoral muscle from a pre-segmented breast region achieving an accuracy of 85% using an unspecified dataset.

Wongthanavas and Tanvoraphonkchai (2008) proposed a two-dimensional cellular automata based segmentation approach for differentiating various tissues inside the mammogram with the images divided into four regions based on their intensity with cellular automata used for refining the edges of each segmented region. However, their method had difficulties in handling images with low contrast and images containing dense breasts. A nonlinear diffusion filtering-based approach for removing the pectoral muscle from a pre-segmented breast region was proposed by Mirzaalian et al. (2007) based on the notion that the nonlinear diffusion filters tend to homogenize different regions in the image without reducing the sharpness of the edges between different image regions. Evaluated using a subset of 90

images from MIAS dataset, their proposed method was claimed to be more accurate than some other methods based on Hough transform and Gabor wavelet techniques. However, they have validated their results based on variance and mean error of Hausdorff distance (Huttenlocher et al. 1993) which are non-standard statistical measures for breast segmentation studies (mostly used for validation of CT/MRI segmentation methods). Kinoshita et al. (2008) proposed a Radon domain-based approach for segmenting the pectoral muscle from mammograms (Radon domain is commonly used for detecting straight lines in an image, similar to the Hough transform). Images are first filtered using Wiener filtering (Gonzalez and Woods 2012) for removing the noise followed by thresholding and morphological operations for removing small background objects such as labels. Then, the breast region is segmented by taking the object with the highest number of connected pixels. The initial pectoral muscle region is selected based on a combination of Canny edge detector and the average region intensity. The image is then transformed to the Radon domain and the lines representing the pectoral muscle boundary are extracted with the slope toward the x -axis being considered between 5° and 50° for the approximation. Evaluated using one of the largest private datasets used for validating the segmentation results containing 1080 mammograms, their method achieved a FP rate of $8.99 \pm 38.72\%$ and a FN rate of $9.13 \pm 11.87\%$.

Yoon et al. (2016) proposed using a random sample consensus (RANSAC) technique for removing the pectoral muscle from a pre-segmented breast region with the CLAHE method being used for enhancing the image contrast. The images are filtered using an oblique kernel capable of locating blurred edges based on the notion that the pectoral muscle boundary can be represented as an oblique diagonal. The filtered image is then converted to binary using Otsu's thresholding method and the edge candidates are detected in the upper half region of the image using a Hough transform. The edge candidates are then chosen based on the location of the chest wall by connecting edge candidates having a range of 100° – 170° for left-MLO images and a range of 280° – 350° for right-MLO images with the longest line being considered as the pectoral muscle boundary. The boundary is then refined by a quadratic curve fitting using non-linear RANSAC method. Evaluated using the MIAS dataset, their proposed method was able to achieve an acceptable segmentation accuracy in 92.2% of images. Alam and Islam (2014) proposed using K-means clustering for removing the pectoral muscle from a pre-segmented breast outline where the tissues inside the breast are clustered using a K-means approach configured to cluster the image into 3 regions. An initial pectoral muscle region is then determined using a morphological selection algorithm based on the assumption that the pectoral muscle region could be (roughly) represented as a triangle with high intensity and a gradual reduction in the width when measured from top to bottom. Evaluated on the mini-MIAS dataset, their proposed method was able to achieve an acceptable accuracy in 90.3% of images according to a visual inspection of the segmented images.

Toz and Erdogmus (2018) proposed using Single Sided Edge Marking (SSEM) technique where geometrical properties and neighborhood relations are used for locating the pectoral muscle region based on the notion that the pectoral muscle is expected to be located near the chest wall, approximately on the left-upper region of the mammogram. In their proposed method, the images are first filtered using a 3×3 median filter followed by biorthogonal wavelet transform with the image contrast enhanced using CLAHE technique. The mammogram noise is then further reduced using an anisotropic diffusion filter and an initial pectoral muscle region is then determined using edge detection performed at angles of 30° – 45° based on the assumption that the pectoral muscle region could be (roughly) represented as a triangle with a high but homogeneous intensity (compared to other breast tissues). The initial pectoral muscle boundary is then refined using linear interpolation for filling any missing boundaries. Evaluated on a subset of 60 images from the INbreast dataset, their proposed method was

able to achieve a mean sensitivity of 95.6%, a FP rate of 2.74% and a FN rate of 4.33%. Shinde and Rao (2019) proposed an approach for removing the pectoral muscle from a pre-segmented breast region using a Support Vector Machine (SVM) based on the assumption that the pectoral muscle is expected to be located near the chest wall approximately on the left-upper region of the mammogram with the noise in the image reduced using a median filter. Then, the initial pectoral muscle region is segmented by three different segmentation methods that include a K-means clustering method using 3 classes, region growing with seed point selected based on assumed pectoral muscle location and region intensity and Otsu's thresholding techniques. Then, statistical and texture features from the initial pectoral muscle region identified by each of the segmentation methods are extracted using Gray Level Co-occurrence Matrix (GLCM) and used in an SVM classifier for determining the best segment corresponding to the pectoral muscle region (with no further refinement of the boundary by refinement methods). While an interesting approach, their proposed method was able to provide acceptable segmentation in 93.7% of the cases evaluated on the mini-MIAS dataset using visual inspection of the accuracy of the segmentation making it comparable (but not more accurate) than other proposed methods. Mughal et al. (2018) proposed using the Prewitt operation based edge detection method coupled with convex hull approximation for removing the pectoral muscle from a pre-segmented breast region. Based on the notion that the pectoral muscle boundary is often vertically oriented, a 3×3 Prewitt filter is used for detecting the edges in the image with morphological closing being used for connecting any disjointed edges. Then, the image is converted to binary and a convex hull connecting the four corners of the binary image is computed. Finally, this convex hull is used for masking the original mammogram where pixels outside the convex hull are considered to represent the pectoral muscle and are discarded while the pixels inside this convex hull are considered as the breast region and are retained. Evaluated using the MIAS dataset and a private dataset containing 20 FFDM images, their proposed method achieved a mean FP rate of 0.99% with FN rate of 5.67% and a mean FP rate of 0.98% with FN rate of 5.66%, respectively. Although the segmentation was acceptable in the majority of images (based on visual inspection), their proposed method had difficulties in segmenting breast with a large portion of the pectoral muscle was visible.

Yin et al. (2018) proposed a level set-based approach for pectoral muscle segmentation based on the notion that the pectoral muscle is expected to be located near the chest wall, approximately on the left-upper region of the mammogram. First, a rectangular area containing the pectoral muscle on the top left corner of the image is defined (similar to the ROI shown in Fig. 12) and cropped from the image. Then, the cropped region is enhanced using a fractional differential method (Chen et al. 2012) followed by an initial segmentation of the pectoral muscle boundary using iterative thresholding. Utilizing the least square method (Boukamp 1986), an approximate curve representing the pectoral muscle boundary is computed and refined using local region-based active contours. In local region-based active contours, the ROI is subdivided to circular regions that act as independent regions around each pixel along the boundary, resulting in a more accurate boundary segmentation at the cost of computational requirements. Evaluated using a private dataset containing 720 FFDM images, their proposed method achieved acceptable segmentation in 94.6% of images with a mean DSC of 0.986. Pavan et al. (2019) proposed an active contour-based approach for pectoral muscle segmentation from FFDM images based on the notion that the pectoral muscle is expected to be located near the chest wall, approximately on the left-upper region of the mammogram. The breast region is segmented using thresholding and the initial pectoral muscle boundary candidates are computed by using a Canny edge detector combined with Hough transform. Then, the strongest edge candidate is selected by a combination of the size

(length) and the orientation of the candidate edges and used in the initialization of an active contour-based approach for refining the final boundary. Evaluated using a private dataset containing 30 images, their proposed method achieved a mean JSC of 0.92.

Based on the assumption that the pectoral muscle is expected to be located in the upper-left region of the image near the chest wall, Slavković-Ilić et al. (2016) proposed a polynomial fitting-based approach for removing the pectoral muscle from mammograms from a pre-segmented breast region. The original images are transformed so that the chest wall would be positioned on the left side of the image. Then, a rectangular ROI is defined using the top 70% of the breast height and width and the image is normalized for enhancing the contrast within this ROI. A three-step k-means clustering approach is then used for detecting an initial pectoral muscle region by clustering the ROI using a K-means method with two, three and four cluster and taking the cluster with the highest mean intensity at each step. The objects in each cluster are then cleaned using mathematical morphology with the initial pectoral muscle region selected based on the size of the segmented objects in each cluster using a custom set of rules. Finally, the boundary is refined by a polynomial fitting method using a third-degree polynomial. Evaluated on the mini-MIAS dataset using visual inspection of the accuracy of the segmentation, their proposed method was able to provide good and acceptable segmentation in 68.32% and 19.25% of the cases, respectively. Rampun et al. (2017) proposed an approach for removing the pectoral muscle from mammograms using contour growing technique. The noise in the mammogram image is reduced using a combination of 9×9 median filtering and anisotropic diffusion filtering with the breast boundary segmented using thresholding and mathematical morphology. Then, a Canny edge detection method is used for extracting the initial pectoral muscle region using a set of custom rules based on the assumption that the pectoral muscle is located near the chest wall approximately on the left-upper region of the mammogram. The final boundary is then refined using a contour growing technique with the seeds defined based on the initial pectoral muscle boundary. Evaluated on the MIAS dataset, their proposed method was able to achieve a DSC of 0.978 and an accuracy of 98.1%.

5.7 Summary

Unlike the breast boundary segmentation, methods proposed for pectoral muscle segmentation are usually more complex as the sole use of intensity is not appropriate for this segmentation. More refined pre-processing steps are required for ensuring an accurate pectoral muscle segmentation as its intensity might not differ significantly compared to other tissues in the breast. Moreover, as was the case with breast boundary segmentation, the quality of the images can be considered as the main factor influencing the accuracy of the segmentation. As a result, many methods have validated their approach using a subset of images in the dataset (again with MIAS and mini-MIAS datasets being the most popular as they have higher quality images compared to DDSM dataset). Moreover, as there is no gold standard for pectoral muscle segmentation, most methods use the manual segmentation by different users/experts as the gold standard in their study or base the segmentation accuracy on a visual inspection of the correctness of the segmentation, making a direct comparison between the performance of these methods difficult. Additionally, many methods work on the assumption that the pectoral muscle is located in the upper-left region of the image near the chest wall. Line estimation methods can be considered as the most popular followed by region growing approaches. However, although region growing methods are able to provide more accurate segmentation, they are sensitive to the initial seed positions while defining

these initial seeding points and stopping criterion for these methods can be difficult. Table 3 shows a comparison between different pectoral muscle segmentation methods.

6 Discussion

A survey of different breast segmentation methods from the literature makes it clear that most methods are designed around the same basic principles. First, the images are usually filtered and smoothed using different filtering techniques with median filters and anisotropic diffusion filters being the most popular and widely used filters. Then, the images are often converted to binary with either a global thresholding approach using a threshold value of 15 to 20 (8-bit images) or by using adaptive thresholding with the Otsu's thresholding method being the most popular. Finally, the breast area is often taken by keeping the object with the largest number of connected pixels. Breast boundary refinement steps might also be included with mathematical morphology-based methods and polynomial fitting being the most popular approaches. Some methods might also include contrast enhancement steps with intensity normalization and CLAHE methods being the most popular. The main issue with CLAHE method, in general, is the fact that not only the contrast of the breast is increased (considered as foreground), but the contrast of the background is also increased (Gupta and Tiwari 2017). This can lead to enhancement of the scanning induced artifacts in the scanned film mammography images (FFDM will not be affected), resulting in possible difficulties in thresholding based approaches. Moreover, most methods segment the breast region by keeping the object with the highest number of connected pixels and setting the intensity value of the remaining pixels to zero. Although this approach seems efficient, it often results in losing the skin-air boundary information as most methods do not perform the necessary pre-processing and/or post-processing steps required for enhancing and keeping this boundary as illustrated in Fig. 14.

Compared to CLAHE enhancement, enhancing the image using Adaptive Gamma Correction with Weighting Distribution (AGCWD) as proposed by Slavković-Ilić et al. (2016) can be considered an effective breast region enhancement/pre-processing step prior to the breast segmentation as it was shown to be able to enhance the breast region with good accuracy as illustrated in Fig. 15. The breast region could then be extracted with good accuracy from images with most methods including thresholding and morphology approaches as these methods can segment the breast region with good accuracy as shown in Table 2.

Another artifact seen in some scanned mammography images is the tape used for holding the mammogram inside the scanner as seen in Fig. 16a. While the removal of the region masked by the tape is considered beneficial, most methods do not include any steps for its removal. The approach proposed by Shi et al. (2018) can be considered as an effective tape removal method that can also be used to remove the inframammary fold with minimal modifications. Their proposed method is based on the notion that the tape artifacts can usually result in areas with high curvature on an otherwise smooth breast boundary as illustrated in Fig. 16c. Sharp breaks in the breast boundary curvature are detected using a 2D curvilinear detection method with the lowest breakpoint in the upper half of the image being taken as the lower tape boundary with all pixels above the horizontal line passing through the point being set to zero as illustrated in Fig. 16d. The same principle can also be used for detecting and removing the inframammary fold in case it is present in the lower half of the mammogram.

A survey of different methods proposed for pectoral muscle segmentation in mammography images shows that there is still room for improvement. While many methods, apart from

Table 3 Comparison between different pectoral muscle segmentation methods

Proposed by	Method used	Method complexity	Dataset (subset of images used)	Accuracy	Other performance measures
Czaplicka and Włodarczyk (2012)	Thresholding	Low	mini-MIAS	98% (visual validation)	Not mentioned
Shrivastava et al. (2017)	Region intensity	Low	MIAS	91.3% (visual validation)	Not mentioned
Sreedevi and Sherty (2015)	Region intensity	Low	mini-MIAS (161)	90.06% (visual validation)	Not mentioned
Chen and Zwigelaar (2012)	Region growing	Medium	mini-MIAS	97.8%	Not mentioned
Maitra et al. (2012)	Region growing	Medium	mini-MIAS	95.65%	Not mentioned
Esener et al. (2018)	Region growing	Medium	MIAS	94.4%	89.62% sensitivity 99.99% specificity
Raba et al. (2005)	Region growing	Medium	mini-MIAS	86% (visual validation)	Not mentioned
Saltanat et al. (2010)	Region growing	Medium	mini-MIAS	92% (visual validation)	Not mentioned
Taghanaki et al. (2017)	Region growing	Medium	MIAS	95%	Not mentioned
Taghanaki et al. (2017)	Region growing	Medium	DDSM	94%	Not mentioned
Hazarika and Mahanta (2018)	Region growing	Medium	mini-MIAS (150)	92%	Not mentioned
Ma et al. (2007)	Graph-cut	High	mini-MIAS (84)	Not mentioned	0.58% FP 5.77% FN
Abdellatif et al. (2019)	Graph-cut	Medium	mini-MIAS (80)	Not mentioned	1.2% FP 20.4% FN
Camilus et al. (2010)	Graph-cut	Medium	mini-MIAS (84)	Not mentioned	0.64% FP 5.58% FN
Camilus et al. (2011)	Watershed	Medium	mini-MIAS (84)	94%	Not mentioned
Weidong and Shunren (2003)	Hough transform	Medium	Unspecified (60)	81.7% (visual validation)	Not mentioned

Table 3 continued

Proposed by	Method used	Method complexity	Dataset (subset of images used)	Accuracy	Other performance measures
Xu et al. (2007)	Hough transform	Medium	Unspecified (52)	Not mentioned	94.5% VO
Ferrari et al. (2004b)	Hough transform	Medium	mini-MIAS (84)	Not mentioned	1.98% FP 25.19% FN
Ferrari et al. (2004b)	Gabor filters	Medium	mini-MIAS (84)	Not mentioned	0.58% FP 5.77% FN
Qayyum and Basit (2016)	Canny edge detection	Medium	mini-MIAS	93% (visual validation)	Not mentioned
Palkar and Agrawal (2016)	Straight line estimation	Low	MIAS	80% (visual validation)	Not mentioned
Chakraborty et al. (2012)	Line estimation and Shape feature	Medium	mini-MIAS (80)	Not mentioned	89.08% VO
Chakraborty et al. (2012)	Line estimation and Shape feature	Medium	FFDM (80)	Not mentioned	89.25% VO
Mustra and Grgic (2013)	Polynomial fitting/Curve estimation	Medium	mini-MIAS	96.6%	Not mentioned
Shen et al. (2018)	Polynomial fitting/Curve estimation	Medium	DDSM (128)	Not mentioned	0.9715 DSC
Shen et al. (2018)	Polynomial fitting/Curve estimation	Medium	mini-MIAS	96.81%	0.9496 DSC
Kwok et al. (2004)	Hough transform and cliff detection	Medium	MIAS	88.8% (visual validation)	Not mentioned
Kwok et al. (2001)	Iterative thresholding and cliff detection	Medium	MIAS	94% (visual validation)	Not mentioned
Sultana et al. (2010)	Mean-shift clustering	Medium	mini-MIAS	Not mentioned	13% FP 84% TP
Li et al. (2013)	Texture features	Medium	mini-MIAS	90%	Not mentioned
Li et al. (2013)	Texture features	Medium	DDSM (100)	92%	Not mentioned
Adel et al. (2007)	Markov random fields	Medium	Unspecified (50)	68% (visual validation)	Not mentioned
Wang et al. (2010)	Markov random fields	High	DDSM (80)	91% (visual validation)	Not mentioned

Table 3 continued

Proposed by	Method used	Method complexity	Dataset (subset of images used)	Accuracy	Other performance measures
Mustra et al. (2009)	Wavelet-based decomposition	Medium	Unspecified	85%	Not mentioned
Slavković-Ilić et al. (2016)	K-means clustering	High	mini-MIAS	87.57% (visual validation)	Not mentioned
Alam and Islam (2014)	K-means clustering	Low	mini-MIAS	90.3% (visual validation)	Not mentioned
Rampun et al. (2017)	Contour growing	Medium	MIAS	98.1%	0.978 DSC
Yin et al. (2018)	Active contours	High	FFDM (720)	94.6%	0.986 DSC
Pavan et al. (2019)	Active contour	Medium	Unspecified (30)	Not mentioned	0.92 JSC
Mughal et al. (2018)	Convex hull	Medium	MIAS	Not mentioned	0.99% FP 5.67% FN
Mughal et al. (2018)	Convex hull	Medium	FFDM (20)	Not mentioned	0.98% FP 5.66% FN
Kinoshita et al. (2008)	Radon domain based line estimation	High	Unspecified (1080)	Not mentioned	8.99 FP 9.13 FN
Yoon et al. (2016)	Curve fitting	High	MIAS	92.2%	Not mentioned
Toz and Erdogmus (2018)	Geometrical properties	High	INbreast (60)	Not mentioned	95.6% sensitivity 2.74% FP 4.33% FN
Shinde and Rao (2019)	Support vector machine (SVM)	High	mini-MIAS	93.7% (visual validation)	Not mentioned

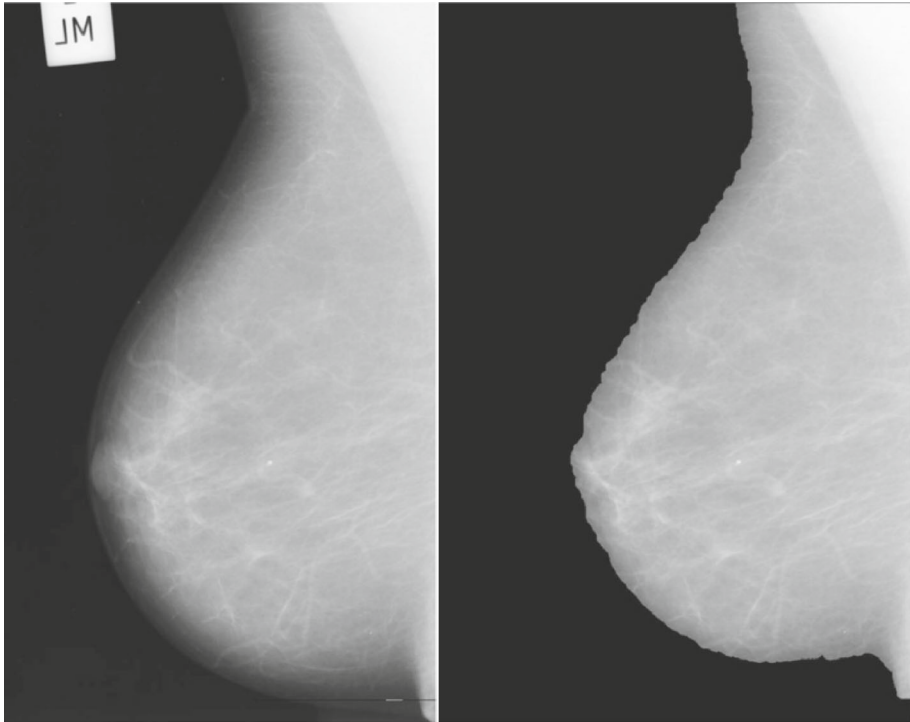


Fig. 14 A sample image from the mini-MIAS dataset and the segmented breast outline (Shen et al. 2018). As seen, the breast outline is not smooth and the air-skin boundary is removed

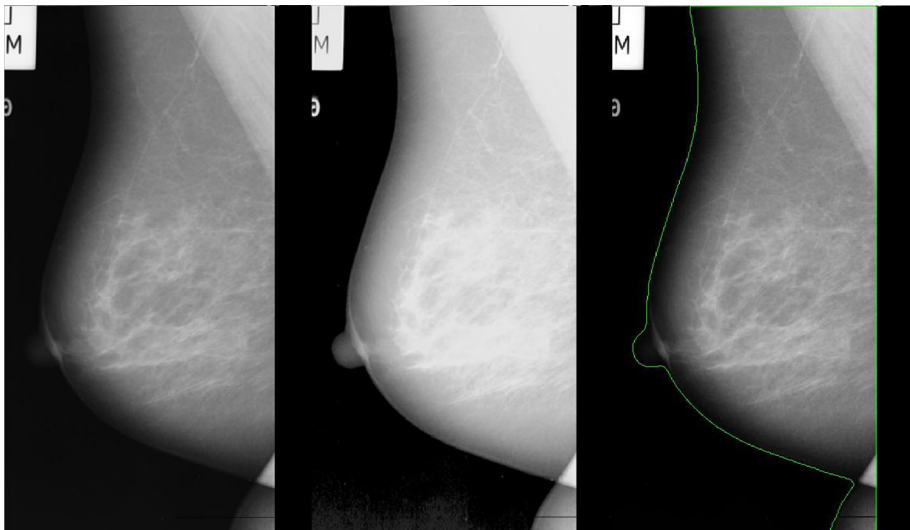


Fig. 15 A sample image from the mini-MIAS dataset and the enhanced breast outline using AGCWD method proposed by Slavković-Ilić et al. (2016). As seen, the breast outline and the air-skin boundary are adequately enhanced and segmented

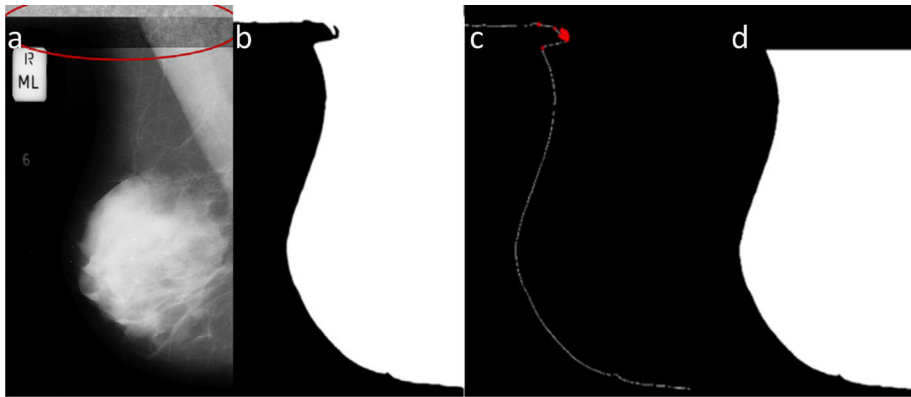


Fig. 16 **a** Sample image with tape artifact, **b** initial breast region, **c** breakpoints in the boundary, **d** final boundary with removed tape artifact (Shi et al. 2018)

thresholding approaches, are capable of achieving an accuracy of 92% or more, they have been mostly validated using a small subset of images from available datasets as illustrated in Table 3. This trend not only makes a comparison between these methods difficult, but it also makes it difficult to assess the performance of these methods when applied to large amounts of data with varying characteristics. Active contours can be considered as one of the most accurate approaches proposed for pectoral muscle segmentation that can result in a good segmentation. However, although active contours have been gaining popularity in medical segmentation tasks and have been shown to provide acceptable segmentation in a wide range of tasks, there are not that many methods that use active contours for pectoral muscle segmentation. Region growing methods (although proper seed placement can be challenging) are also capable of segmenting pectoral muscle region with good accuracy as the method proposed by Taghanaki et al. (2017) was able to segment the pectoral muscle region with 94% accuracy when applied to the entire DDSM dataset, considering the size of the dataset and possible variations in image characteristics, this is indeed an excellent performance. While most of the pectoral muscle segmentation methods do not include any contrast enhancement steps, the inclusion of CLAHE (or its derivatives) seems to increase the accuracy of muscle boundary detection. Methods proposed by Mustra and Grgic (2013), Rampun et al. (2017), Shen et al. (2018) and Taghanaki et al. (2017) can be considered as some of the best approaches proposed for pectoral muscle segmentation as they are able to cope with images with vague boundaries and are capable of providing acceptable segmentation in most images with Fig. 17 illustrating the segmentation by these methods.

7 Conclusions

In this paper, various methods proposed for breast boundary and pectoral muscle segmentation (from MLO images) using FFDM and SFM mammograms were discussed and compared, but there is no single method that can work well for segmenting the breast boundary or the pectoral muscle regions. A survey of different segmentation methods from the literature makes it clear that most methods are designed around the same basic principles with thresholding being the main concept in breast region segmentation and curve estimation being the main concept in pectoral muscle segmentation. Moreover, median filtering can be considered as the most

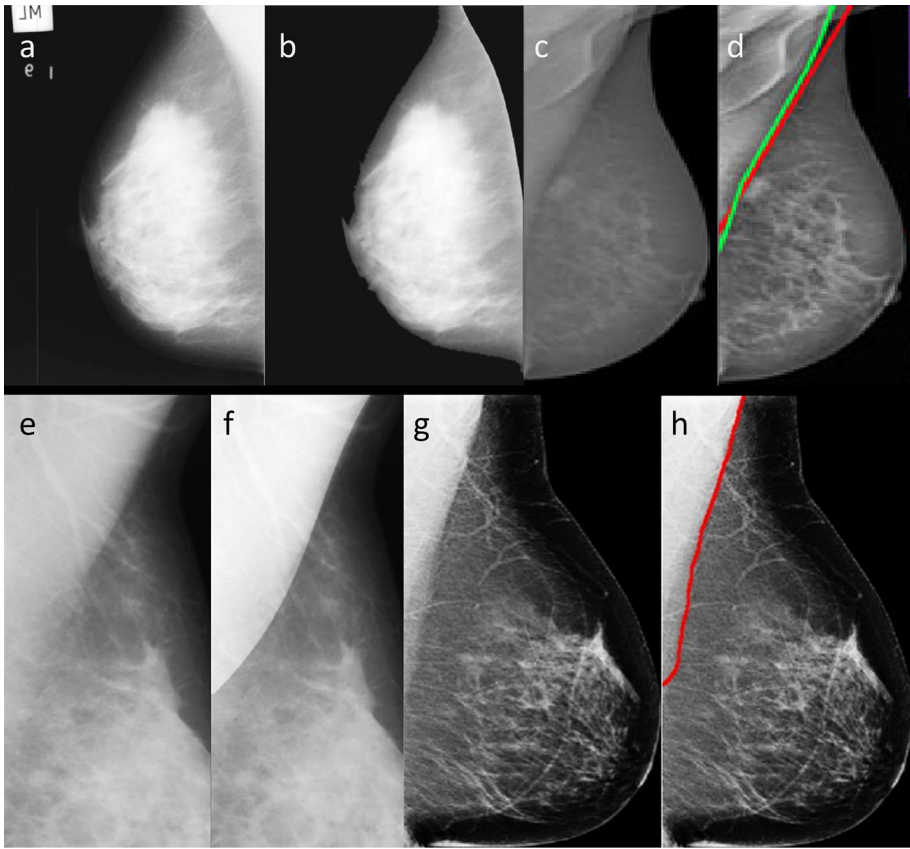


Fig. 17 **a, b** segmentation of a sample image by Shen et al. (2018); **c, d** segmentation of a sample image by Taghanaki et al. (2017) with green line representing ground truth and red line representing their proposed segmentation; **e, f** segmentation of a sample image by Mustra and Grgic (2013) and **g, h** segmentation of a sample image by Taghanaki et al. (2017). (Color figure online)

popular noise reduction method in the literature with mathematical morphology often used for smoothing the segmented boundary. While breast boundary segmentation has received a large interest from researchers with the majority of proposed methods achieving an accuracy of more than 95%, pectoral muscle segmentation remains a challenging task (with many methods having an accuracy under 95%) that requires further investigation and development as it can be considered as one of the preliminary steps in computer-aided detection/diagnosis of breast cancer as the pectoral muscle region can be easily be mistaken for abnormalities by CAD systems.

Compliance with ethical standards

Conflict of interest The authors have no conflict of interests to declare.

References

- Abdellatif H, Taha T, Zahran O, Al-Nauimy W, El-Samie FA (2019) K2. Automatic pectoral muscle boundary detection in mammograms using eigenvectors segmentation. In: 2012 29th national radio science conference (NRSC), 2012. IEEE, pp 633–640
- Adel M, Rasigni M, Bourennane S, Juhan V (2007) Statistical segmentation of regions of interest on a mammographic image. *EURASIP J Adv Signal Process* 2007:3
- Alam N, Islam MJ (2014) Pectoral muscle elimination on mammogram using K-means clustering approach. *Int J Comput Vis Signal Process* 4:11–21
- Ancy C, Nair LS (2018) Tumour classification in graph-cut segmented mammograms using GLCM features-based SVM. In: *Intelligent engineering informatics*. Springer, pp 197–208
- Bajaj V, Pawar M, Meena VK, Kumar M, Sengur A, Guo Y (2017) Computer-aided diagnosis of breast cancer using bi-dimensional empirical mode decomposition. *Neural Comput Appl*. <https://doi.org/10.1007/s00521-017-3282-3>
- Ballard DH (1987) Generalizing the Hough transform to detect arbitrary shapes. In: *Readings in computer vision*. Elsevier, pp 714–725
- Boukamp BA (1986) A nonlinear least squares fit procedure for analysis of impedance data of electrochemical systems. *Solid State Ionics* 20:31–44
- Camilus KS, Govindan V, Sathidevi P (2010) Computer-aided identification of the pectoral muscle in digitized mammograms. *J Digit Imaging* 23:562–580
- Camilus KS, Govindan V, Sathidevi P (2011) Pectoral muscle identification in mammograms. *J Appl Clin Med Phys* 12:215–230
- Canny J (1986) Computational approach to edge detection. *IEEE Trans Pattern Anal Mach Intell* 8:679–698
- Caselles V, Kimmel R, Sapiro G (1997) Geodesic active contours. *Int J Comput Vis* 22:61–79
- Casti P, Mencattini A, Salmeri M, Ancona A, Mangeri F, Pepe ML, Rangayyan RM (2013) Estimation of the breast skin-line in mammograms using multidirectional Gabor filters. *Comput Biol Med* 43:1870–1881
- Chakraborty J, Mukhopadhyay S, Singla V, Khandelwal N, Bhattacharyya P (2012) Automatic detection of pectoral muscle using average gradient and shape based feature. *J Digit Imaging* 25:387–399
- Chan TF, Vese LA (2001) Active contours without edges. *IEEE Trans Image Process* 10:266–277
- Chen Z, Zwiggelaar R (2012) A combined method for automatic identification of the breast boundary in mammograms. In: 2012 5th international conference on biomedical engineering and informatics (BMEI), 2012. IEEE, pp 121–125
- Chen D, Chen Y, Xue D, Pan F (2012) Adaptive image enhancement based on fractional differential mask. In: 2012 24th Chinese control and decision conference (CCDC), 2012. IEEE, pp 1043–1047
- Christoyianni I, Koutras A, Dermatas E, Kokkinakis G (2002) Computer aided diagnosis of breast cancer in digitized mammograms. *Comput Med Imaging Graph* 26:309–319
- Clark K et al (2013) The Cancer Imaging Archive (TCIA): maintaining and operating a public information repository. *J Digit Imaging* 26:1045–1057
- Collins W (1956) Observation of growth rates of human tumors. *Am J Roentgenol* 76:988
- Czaplicka K, Włodarczyk H (2012) Automatic breast-line and pectoral muscle segmentation. *Schedae Inform* 2011:195–209
- Deserno T, Soiron M, Oliveira J, Araujo A (2011) Towards computer-aided diagnostics of screening mammography using content-based image retrieval. In: 2011 24th SIBGRAPI conference on graphics, patterns and images (Sibgrapi), 2011. IEEE, pp 211–219
- Doi K (2007) Computer-aided diagnosis in medical imaging: historical review, current status and future potential. *Comput Med Imaging Graph* 31:198–211
- D'orsi C, Bassett L, Feig S (1998) Breast imaging reporting and data system (BI-RADS) Breast imaging atlas, 4th edn. American College of Radiology, Reston
- Elshinawy MY, Abdelmageed WW, Badawy A-HA, Chouikha MF (2010) Pre-CAD system for normal mammogram detection using local binary pattern features. In: 2010 IEEE 23rd international symposium on computer-based medical systems (CBMS), 2010. IEEE, pp 352–357
- Ergin S, Esener II, Yüksel T (2016) A genuine GLCM-based feature extraction for breast tissue classification on mammograms. *Int J Intell Syst Appl Eng* 4:124–129
- Esener II, Ergin S, Yüksel T (2018) A novel multistage system for the detection and removal of pectoral muscles in mammograms. *Turk J Electr Eng Comput Sci* 26:35–49
- Ferrari R, Frere A, Rangayyan R, Desautels J, Borges R (2004a) Identification of the breast boundary in mammograms using active contour models. *Med Biol Eng Comput* 42:201–208
- Ferrari RJ, Rangayyan RM, Desautels JL, Borges R, Frere AF (2004b) Automatic identification of the pectoral muscle in mammograms. *IEEE Trans Med Imaging* 23:232–245

- Ganesan K, Acharya UR, Chua KC, Min LC, Abraham KT (2013) Pectoral muscle segmentation: a review. *Comput Methods Programs Biomed* 110:48–57
- Gonzalez RC, Woods RE (2012) *Digital image processing*. Prentice Hall, Upper Saddle River
- Gupta B, Tiwari M (2017) A tool supported approach for brightness preserving contrast enhancement and mass segmentation of mammogram images using histogram modified grey relational analysis. *Multidimens Syst Signal Process* 28:1549–1567
- Hammouche K, Diaf M, Siarry P (2008) A multilevel automatic thresholding method based on a genetic algorithm for a fast image segmentation. *Comput Vis Image Underst* 109:163–175
- Hazarika M, Mahanta LB (2018) A novel region growing based method to remove pectoral muscle from MLO mammogram images. In: *Advances in electronics, communication and computing*. Springer, pp 307–316
- Heath M, Bowyer K, Kopans D, Kegelmeyer P, Moore R, Chang K, Munishkumaran S (1998) Current status of the digital database for screening mammography. In: *Digital mammography*. Springer, pp 457–460
- Huang S-C, Cheng F-C, Chiu Y-S (2013) Efficient contrast enhancement using adaptive gamma correction with weighting distribution. *IEEE Trans Image Process* 22:1032–1041
- Huttenlocher DP, Klanderman GA, Rucklidge WJ (1993) Comparing images using the Hausdorff distance. *IEEE Trans Pattern Anal Mach Intell* 15:850–863
- Ibrahim NSA, Soliman NF, Abdallah M, El-Samie FEA (2016) An algorithm for pre-processing and segmentation of mammogram images. In: *2016 11th international conference on computer engineering and systems (ICCES)*, 2016. IEEE, pp 187–190
- Karnan M, Thangavel K (2007) Automatic detection of the breast border and nipple position on digital mammograms using genetic algorithm for asymmetry approach to detection of microcalcifications. *Comput Methods Programs Biomed* 87:12–20
- Kinoshita SK, Azevedo-Marques PM, Pereira RR, Rodrigues JAH, Rangayyan RM (2008) Radon-domain detection of the nipple and the pectoral muscle in mammograms. *J Digit Imaging* 21:37–49
- Kwan ML et al (2009) Epidemiology of breast cancer subtypes in two prospective cohort studies of breast cancer survivors. *Breast Cancer Res* 11:R31
- Kwok S, Chandrasekhar R, Attikiouzel Y (2001) Automatic pectoral muscle segmentation on mammograms by straight line estimation and cliff detection. In: *intelligent information systems conference, The Seventh Australian and New Zealand 2001, 2001*. IEEE, pp 67–72
- Kwok SM, Chandrasekhar R, Attikiouzel Y, Rickard MT (2004) Automatic pectoral muscle segmentation on mediolateral oblique view mammograms. *IEEE Trans Med Imaging* 23:1129–1140
- Lancaster P, Salkauskas K (1986) *Curve and surface fitting: an introduction*. Academic press
- Lewin JM et al (2001) Comparison of full-field digital mammography with screen-film mammography for cancer detection: results of 4,945 paired examinations. *Radiology* 218:873–880
- Li Y, Chen H, Yang Y, Yang N (2013) Pectoral muscle segmentation in mammograms based on homogenous texture and intensity deviation. *Pattern Recogn* 46:681–691
- Linguraru MG, Marias K, English R, Brady M (2006) A biologically inspired algorithm for microcalcification cluster detection. *Med Image Anal* 10:850–862
- Liu L, Wang J, Wang T (2011) Breast and pectoral muscle contours detection based on goodness of fit measure. In: *2011 5th international conference on bioinformatics and biomedical engineering, (ICBBE)*, 2011. IEEE, pp 1–4
- Lopez MG et al (2012) BCDR: a breast cancer digital repository. In: *15th international conference on experimental mechanics*, 2012. BCDR dataset accessible at <https://bcdr.eu/information/about>. Accessed 29 May 2019
- Ma F, Bajger M, Slavotinek JP, Bottema MJ (2007) Two graph theory based methods for identifying the pectoral muscle in mammograms. *Pattern Recogn* 40:2592–2602
- Maitra IK, Nag S, Bandyopadhyay SK (2012) Technique for pre-processing of digital mammogram. *Comput Methods Programs Biomed* 107:175–188
- Martí R, Oliver A, Raba D, Freixenet J (2007) Breast skin-line segmentation using contour growing. In: *Iberian conference on pattern recognition and image analysis, 2007*. Springer, pp 564–571
- Marx C, Malich A, Facius M, Grebenstein U, Sauner D, Pfeleiderer SO, Kaiser WA (2004) Are unnecessary follow-up procedures induced by computer-aided diagnosis (CAD) in mammography? Comparison of mammographic diagnosis with and without use of CAD. *Eur J Radiol* 51:66–72
- Matheus BRN, Schiabel H (2011) Online mammographic images database for development and comparison of CAD schemes. *J Digit Imaging* 24:500–506
- Mirzaalian H, Ahmadzadeh MR, Sadri S, Jafari M (2007) Pre-processing algorithms on digital mammograms. In: *MVA, 2007*, pp 118–121
- Moghbel M, Mashohor S (2013) A review of computer assisted detection/diagnosis (CAD) in breast thermography for breast cancer detection. *Artif Intell Rev* 39:305–313

- Moreira IC, Amaral I, Domingues I, Cardoso A, Cardoso MJ, Cardoso JS (2012) Inbreast: toward a full-field digital mammographic database. *Acad Radiol* 19:236–248
- Mughal B, Muhammad N, Sharif M, Rehman A, Saba TJBC (2018) Removal of pectoral muscle based on topographic map and shape-shifting silhouette. *BMC Cancer* 18:778
- Mustra M, Grgic M (2013) Robust automatic breast and pectoral muscle segmentation from scanned mammograms. *Signal Process* 93:2817–2827
- Mustra M, Bozek J, Grgic M (2009) Breast border extraction and pectoral muscle detection using wavelet decomposition. In: EUROCON 2009, EUROCON'09. IEEE, 2009. IEEE, pp 1426–1433
- Mustra M, Grgic M, Rangayyan RMJM (2016) Review of recent advances in segmentation of the breast boundary and the pectoral muscle in mammograms. *Med Biol Eng Comput* 54:1003–1024
- Nagi J, Kareem SA, Nagi F, Ahmed SK (2010) Automated breast profile segmentation for ROI detection using digital mammograms. In: 2010 IEEE EMBS conference on biomedical engineering and sciences (IECBES), 2010. IEEE, pp 87–92
- Nayak T, Bhat N, Bhat V, Shetty S, Javed M, Nagabhushan P (2019) Automatic segmentation and breast density estimation for cancer detection using an efficient watershed algorithm. In: Data analytics and learning. Springer, pp 347–358
- Nazaré J, de Carvalho Filho AO, Silva AC, De Paiva AC, Gattass M (2015) Automatic detection of masses in mammograms using quality threshold clustering, correlogram function, and SVM. *J Digit Imaging* 28:323–337
- Osher S, Fedkiw R (2006) Level set methods and dynamic implicit surfaces, vol 153. Springer, Berlin
- Otsu N (1979) A threshold selection method from gray-level histograms. *IEEE Trans Syst Man Cybern* 9:62–66
- Palkar P, Agrawal DP (2016) A technique to extract statistical parameters of digital mammogram to detect breast cancer. *Int J Adv Res Sci Eng Technol* 3(12):3033–3038
- Pavan AL, Vacavant A, Alves AF, Trindade AP, de Pina DR (2019) Automatic identification and extraction of pectoral muscle in digital mammography. In: World congress on medical physics and biomedical engineering 2018. Springer, pp 151–154
- Qayyum A, Basit A (2016) Automatic breast segmentation and cancer detection via SVM in mammograms. In: 2016 international conference on emerging technologies (ICET), 2016. IEEE, pp 1–6
- Quellec G, Lamard M, Cozic M, Coatrieux G, Cazuguel G (2016) Multiple-instance learning for anomaly detection in digital mammography. *IEEE Trans Med Imaging* 35:1604–1614
- Raba D, Oliver A, Martí J, Peracaula M, Espunya J (2005) Breast segmentation with pectoral muscle suppression on digital mammograms. In: Iberian conference on pattern recognition and image analysis, 2005. Springer, pp 471–478
- Rampun A, Morrow PJ, Scotney BW, Winder J (2017) Fully automated breast boundary and pectoral muscle segmentation in mammograms. *Artif Intell Med* 79:28–41
- Rickard HE, Tourassi GD, Eltonsy N, Elmaghraby AS (2004) Breast segmentation in screening mammograms using multiscale analysis and self-organizing maps. In: 26th Annual International Conference of the IEEE Engineering in Medicine and Biology Society, 2004. IEMBS'04. IEEE, pp 1786–1789
- Saidin N, Ngah UK, Sakim HAM, Siang DN, Hoe MK, Shuaib IL (2010) Density based breast segmentation for mammograms using graph cut and seed based region growing techniques. In: 2010 2nd international conference on computer research and development, 2010. IEEE, pp 246–250
- Salama MS, Eltrass AS, Elkamchouchi HM (2018) An improved approach for computer-aided diagnosis of breast cancer in digital mammography. In: 2018 IEEE international symposium on medical measurements and applications (MeMeA), 2018. IEEE, pp 1–5
- Saltanat N, Hossain MA, Alam MS (2010) An efficient pixel value based mapping scheme to delineate pectoral muscle from mammograms. In: 2010 IEEE 5th international conference on bio-inspired computing: theories and applications (BIC-TA), 2010. IEEE, pp 1510–1517
- Sampaio WB, Diniz EM, Silva AC, De Paiva AC, Gattass M (2011) Detection of masses in mammogram images using CNN, geostatistic functions and SVM. *Comput Biol Med* 41:653–664
- Sampat MP, Markey MK, Bovik AC (2005) Computer-aided detection and diagnosis in mammography. *Handb Image Video Process* 2:1195–1217
- Sasikala S, Ezhilarasi M (2018) Fusion of k-Gabor features from medio-lateral-oblique and craniocaudal view mammograms for improved breast cancer diagnosis. *J Cancer Res Ther* 14:1036
- Scheunders P (1996) A genetic Lloyd–Max image quantization algorithm. *Pattern Recogn Lett* 17:547–556
- Selvathi D, Poornila AA (2018) Deep learning techniques for breast cancer detection using medical image analysis. In: Biologically rationalized computing techniques for image processing applications. Springer, pp 159–186
- Senthilkumar B, Umamaheshwari G (2011) A review on computer aided detection and diagnosis-towards the treatment of breast cancer. *Eur J Sci Res* 52:437–452

- Shen R, Yan K, Xiao F, Chang J, Jiang C, Zhou K (2018) Automatic pectoral muscle region segmentation in mammograms using genetic algorithm and morphological selection. *J Digit Imaging* 31:680–691
- Shi P, Zhong J, Rampun A, Wang H (2018) A hierarchical pipeline for breast boundary segmentation and calcification detection in mammograms. *Comput Biol Med* 96:178–188
- Shinde V, Rao BT (2019) Novel approach to segment the pectoral muscle in the mammograms. In: *Cognitive informatics and soft computing*. Springer, pp 227–237
- Shrivastava A, Chaudhary A, Kulshreshtha D, Singh VP, Srivastava R (2017) Automated digital mammogram segmentation using dispersed region growing and sliding window algorithm. In: *2017 2nd international conference on image, vision and computing (ICIVC)*, 2017. IEEE, pp 366–370
- Slavković-Ilić M, Gavrovska A, Milivojević M, Reljin I, Reljin B (2016) Breast region segmentation and pectoral muscle removal in mammograms. *Telfor J* 8:50–55
- Sreedevi S, Sherly E (2015) A novel approach for removal of pectoral muscles in digital mammogram. *Procedia Comput Sci* 46:1724–1731
- Subashini T, Ramalingam V, Palanivel S (2010) Pectoral muscle removal and detection of masses in digital mammogram using CCL. *Int J Comput Appl* 1:71–76
- Suckling J et al (1994) The mammographic image analysis society digital mammogram database. In: *Exerpta Medica. International congress series*, 1994. pp 375–378, MIAS dataset accessible at <https://www.repository.cam.ac.uk/handle/1810/250394> and mini-MIAS dataset accessible at <http://peipa.essex.ac.uk/info/mias.html>. Accessed 29 May 2019
- Sultana A, Ciuc M, Strungaru R (2010) Detection of pectoral muscle in mammograms using a mean-shift segmentation approach. In: *2010 8th International conference on communications (COMM)*, 2010. IEEE, pp 165–168
- Taghanaki SA, Liu Y, Miles B, Hamarneh G (2017) Geometry-based pectoral muscle segmentation from MLO mammogram views. *IEEE Trans Biomed Eng* 64:2662–2671
- Tang J, Rangayyan RM, Xu J, El Naqa I, Yang Y (2009) Computer-aided detection and diagnosis of breast cancer with mammography: recent advances. *IEEE Trans Inf Technol Biomed* 13:236–251
- Tayel M, Mohsen A (2010) Breast boarder boundaries extraction using statistical properties of mammogram. In: *2010 IEEE 10th international conference on signal processing (ICSP)*, 2010. IEEE, pp 2468–2471
- Torres GF, Pertuz S (2017) Automatic detection of the retroareolar region in X-ray mammography images. In: *VII Latin American congress on biomedical engineering CLAIB 2016*, Bucaramanga, Santander, Colombia, 26–28 Oct, 2016, 2017. Springer, pp 157–160
- Toz G, Erdogmus P (2018) A single sided edge marking method for detecting pectoral muscle in digital mammograms. *Eng Technol Appl Sci Res* 8:2367–2373
- Tzikopoulos S, Georgiou H, Mavroforakis M, Dimitropoulos N, Theodoridis S (2009) A fully automated complete segmentation scheme for mammograms. In: *2009 16th international conference on digital signal processing*, 2009. IEEE, pp 1–6
- Unni A, Eg N, Vinod S, Nair LS (2018) Tumour detection in double threshold segmented mammograms using optimized GLCM features fed SVM. In: *2018 international conference on advances in computing, communications and informatics (ICACCI)*, 2018. IEEE, pp 554–559
- Wang L, Zhu M-I, Deng L, Yuan X (2010) Automatic pectoral muscle boundary detection in mammograms based on Markov chain and active contour model. *J Zhejiang Univ Sci C* 11:111–118
- Wei K, Guangzhi W, Hui D (2006) Segmentation of the breast region in mammograms using watershed transformation. In: *27th annual international conference of the engineering in medicine and biology society*, 2005. IEEE-EMBS 2005, 2006. IEEE, pp 6500–6503
- Weidong X, Shunren X (2003) A model based algorithm to segment the pectoral muscle in mammograms. In: *Proceedings of the 2003 international conference on neural networks and signal processing*, 2003. IEEE, pp 1163–1169
- Wirth MA, Stapinski A (2003) Segmentation of the breast region in mammograms using active contours. In: *Visual communications and image processing 2003*, 2003. International Society for Optics and Photonics, pp 1995–2007
- Wirth M, Lyon J, Nikitenko D (2004) A fuzzy approach to segmenting the breast region in mammograms. In: *IEEE annual meeting of the fuzzy information*, 2004. Processing NAFIPS'04, 2004. IEEE, pp 474–479
- Wongthanavasus S, Tanvoraphonkchai S (2008) Cellular automata-based identification of the pectoral muscle in mammograms. In: *Proceedings of ISBME 2008 3rd international symposium on biomedical engineering*, 2008. pp 294–298
- Xie W, Li Y, Ma Y (2016a) Breast mass classification in digital mammography based on extreme learning machine. *Neurocomputing* 173:930–941
- Xie W, Li Y, Ma Y (2016b) Breast mass classification in digital mammography based on extreme learning machine. *Neurocomputing* 173:930–941

- Xu W, Li L, Liu W (2007) A novel pectoral muscle segmentation algorithm based on polyline fitting and elastic thread approaching. In: The 1st international conference on bioinformatics and biomedical engineering, 2007. ICBBE 2007, 2007. IEEE, pp 837–840
- Yapa RD, Harada K (2008) Breast skin-line estimation and breast segmentation in mammograms using fast-marching method. *Int J Biol Biomed Med Sci* 3:54–62
- Yin K, Yan S, Song C, Zheng B (2018) A robust method for segmenting pectoral muscle in mediolateral oblique (MLO) mammograms. *Int J Comput Assist Radiol Surg* 14(2):237–248
- Yoon WB, Oh JE, Chae EY, Kim HH, Lee SY, Kim KG (2016) Automatic detection of pectoral muscle region for computer-aided diagnosis using MIAS mammograms. *BioMed Res Int*. <https://doi.org/10.1155/2016/5967580>
- Zhang DH, Heffernan PB, Bucci M, Huo Z (2007) Digital mammography system with improved workflow. Google patents
- Zhang Z, Lu J, Yip YJ (2010) Automatic segmentation for breast skin-line. In: 2010 IEEE 10th international conference on computer and information technology (CIT), 2010. IEEE, pp 1599–1604
- Zhou W, Lv G, Wang L (2017) An automatic breast mass segmentation algorithm in digital mammography. In: 2017 IEEE international conference on signal processing, communications and computing (ICSPCC), 2017. IEEE, pp 1–5

Publisher's Note Springer Nature remains neutral with regard to jurisdictional claims in published maps and institutional affiliations.